Natural diversity in daily rhythms of gene expression contributes to phenotypic variation

Amaury de Montaigu[a], Antonis Giakountis[a,1], Matthew Rubin[b], Réka Tóth[a,2], Frédéric Cremer[a], Vladislava Sokolova[a], Aimone Porri[a], Matthieu Reymond[a,3], Cynthia Weinig[b], and George Coupland[a,4]

[a]Max Planck Institute for Plant Breeding Research, D-50829 Cologne, Germany; and [b]Department of Botany, University of Wyoming, Laramie, WY 82071

Contributed by George Coupland, November 26, 2014 (sent for review May 11, 2014; reviewed by Carlos Alonso-Blanco and Alex A. R. Webb)

Daily rhythms of gene expression provide a benefit to most organisms by ensuring that biological processes are activated at the optimal time of day. Although temporal patterns of expression control plant traits of agricultural importance, how natural genetic variation modifies these patterns during the day and how precisely these patterns influence phenotypes is poorly understood. The circadian clock regulates the timing of gene expression, and natural variation in circadian rhythms has been described, but circadian rhythms are measured in artificial continuous conditions that do not reflect the complexity of biologically relevant day/night cycles. By studying transcriptional rhythms of the evening-expressed gene *GIGANTEA* (*GI*) at high temporal resolution and during day/night cycles, we show that natural variation in the timing of *GI* expression occurs mostly under long days in 77 *Arabidopsis* accessions. This variation is explained by natural alleles that alter light sensitivity of *GI*, specifically in the evening, and that act at least partly independent of circadian rhythms. Natural alleles induce precise changes in the temporal waveform of *GI* expression, and these changes have detectable effects on *PHYTOCHROME INTERACTING FACTOR 4* expression and growth. Our findings provide a paradigm for how natural alleles act within day/night cycles to precisely modify temporal gene expression waveforms and cause phenotypic diversity. Such alleles could confer an advantage by adjusting the activity of temporally regulated processes without severely disrupting the circadian system.

diurnal | circadian | rhythms | Arabidopsis | GIGANTEA

In plants, many aspects of physiology and development, including metabolism, growth, flowering, and plant defense, are controlled by genes whose expression pattern oscillates on a daily basis (1, 2). These genes usually show peaks of expression around the time at which their function is required to regulate downstream processes. The timing of expression of most temporally regulated genes is at least partly determined by the circadian clock, an endogenous time-keeping mechanism that generates internal rhythms of ∼24 h (3). When synchronized to the external day/night cycle, circadian clocks confer an advantage to plants and other organisms by improving fitness (4, 5). Importantly, circadian rhythms are generally studied under conditions of continuous light (LL) or continuous dark (DD), in which they are not influenced by environmental transitions. These constant conditions, however, do not reflect the complexity of biologically relevant day/night cycles that organisms experience in nature. During the day, fluctuations in external cues such as light and temperature also contribute to defining the timing and amplitude of biologic processes. These cues influence rhythms of gene expression either indirectly, by synchronizing endogenous circadian rhythms to the external day/night cycle (6–8), and/or directly, by activating signaling pathways that regulate transcription (9–11). Thus, the precise timing and amplitude of daily gene expression patterns are defined by a combination of endogenous and external signals.

Temporal rhythms of expression control plant traits of ecological and agricultural importance (12–16), and understanding how precisely these rhythms vary and how this variation influences phenotypes has broad implications for plant biology. Natural diversity in daily transcriptional rhythms has mostly been analyzed by comparing gene expression between limited numbers of selected genotypes and by using temporal resolutions of relatively low precision (14, 17). To date, there has been no extensive survey describing how rhythms of expression vary at the intraspecies level, at more informative temporal resolutions, and during biologically relevant day/night cycles. The latter point is of particular relevance because natural variation in rhythms has mainly been studied in artificial continuous conditions that are used to determine certain circadian parameters. Natural variation of period length, defined as the length of the circadian cycle, was quantified in constant environmental conditions by measuring rhythms of leaf movements or oscillations of gene expression (4, 18–21). Phase, or the time at which an event occurs within a cycle, also varies extensively when determined in constant conditions (4, 22). Although changes in period length would be expected to influence phase, the relationship between both parameters is still unclear in natural genotypes (4). In summary, it is not known how much daily rhythms of expression vary in natural genotypes, what mechanisms generate this variation, and to what extent this variation influences phenotypic outputs.

Significance

Daily rhythms of gene expression ensure that biological processes occur at the optimal time of day. In plants, temporally regulated processes include traits of ecological and agricultural importance, and understanding how changes in daily rhythms of expression modify such traits has broad implications. We find that natural genetic variation can accurately modify temporal gene expression waveforms during the day by influencing light signaling pathways, rather than circadian rhythms. We further show that changes in transcriptional patterns induced by natural alleles are sufficient to affect downstream molecular outputs and cause phenotypic diversity. Such natural alleles could provide an advantage by adjusting the activity of temporally regulated processes while avoiding the pleiotropic effects associated with severe disruptions of the circadian system.

Author contributions: A.d.M., C.W., and G.C. designed research; A.d.M., A.G., M. Rubin, R.T., F.C., V.S., and A.P. performed research; A.d.M., A.G., M. Rubin, and M. Reymond analyzed data; and A.d.M. and G.C. wrote the paper.

The authors declare no conflict of interest.

Reviewers: C.A.-B., Centro Nacional de Biotecnología; and A.A.R.W., University of Cambridge.

Freely available online through the PNAS open access option.

[1]Present address: Institute of Molecular Oncology/Molecular Biology and Genetics, B.S.R.C. Alexander Fleming, 16672 Athens, Greece.

[2]Present address: Department of Plant Sciences, University of Oxford, Oxford, OX1 3RB, United Kingdom.

[3]Present address: Institut Jean-Pierre Bourgin, UMR1318 Institut National de Recherche Agronomique/AgroParisTech, INRA Centre de Versailles-Grignon, 78026 Versailles, France.

[4]To whom correspondence should be addressed. Email: coupland@mpipz.mpg.de.

This article contains supporting information online at www.pnas.org/lookup/suppl/doi:10.1073/pnas.1422242112/-/DCSupplemental.

These questions were addressed by using *GIGANTEA* (*GI*) as a model temporally regulated gene. *GI* is conserved within the plant kingdom and regulates a variety of phenotypes such as growth of the hypocotyl, flowering time, cold resistance, and starch accumulation (23–29). The peak of *GI* expression occurs in the evening in various plant species and is regulated by the circadian clock (12, 25, 26, 30–32). To monitor *GI* expression at high temporal resolution and in a large number of genotypes, we fused a 2.5-Kb fragment of the *GI* promoter to the luciferase (*LUC*) marker gene. Similar *GI::LUC* fusions had already been shown to faithfully track the rhythmic expression pattern of the endogenous transcript (33–35). With the luciferase system, we could accurately determine the timing of *GI* expression during day/night cycles and detect genetic loci that cause precise changes in the *GI* expression waveform. This genetic information was then exploited to create lines that precisely differ in their *GI* expression patterns and to test whether changes in these patterns affect downstream phenotypes.

Results and Discussion

Natural Genetic Variation Regulates the Timing of *GI* Expression Within Long-Day Cycles. Natural variation in the waveform of *GI* transcription was tested for by introducing *GI::LUC* into 77 *Arabidopsis* accessions. Temporal patterns of luciferase activity were recorded under five day lengths and used to determine the peak time of *GI::LUC* expression (*GI* peak time, or sidereal phase) in each accession and condition. *GI* peak time varied in all day lengths, but the range of peak times was broader in long photoperiods, and the genetic contribution to peak time variation was more significant in long days (LDs) compared with in short days (SDs) (Fig. 1*A* and *SI Appendix*, Fig. S1 and Tables S1 and S2). *GI* peak times measured in LDs of 16 h strongly correlated with peak times measured in LDs of 14 h and LDs of 12 h, but not as strongly with peak times measured in SDs (Fig. 1*B*). These data suggest the existence of mechanisms that cause variability in the timing of *GI* expression specifically in LDs.

Daily patterns of gene expression are controlled by endogenous and environmental inputs. Pathways that convey information from these internal or external signals could therefore contribute to the day length-dependent variation of *GI* peak time observed in the accessions. External light signals, on the one hand, directly influence the timing of *GI* expression in the evening because an extension of the light period after dusk in SDs is sufficient to cause an immediate delay in *GI* peak time (*SI Appendix*, Fig. S2*A*). The earlier onset of darkness in SDs might explain why *GI* expression and other rhythms are advanced in SDs compared with LDs (Fig. 1*A*) (9, 26, 36) and might also explain why natural variation of *GI* peak time is limited under SDs (Fig. 1*A* and *SI Appendix*, *SI Discussion*). Endogenous circadian rhythms, on the other hand, did not seem to be related to *GI* peak time variation in any of the photoperiods (*SI Appendix*, Fig. S2 *B* and *C* and *SI Discussion*). Circadian rhythms measured in LL do not correlate with phase in *Arabidopsis* accessions (4), and we report a similar trend for *GI* peak time and period length measured in DD, where circadian rhythms are not influenced by light (Fig. 1*B*). Although these results do not exclude that period length influences phase in particular accessions (*SI Appendix*, Fig. S2*D*), they do suggest that natural variation of *GI* peak time in LDs might generally be determined by natural alleles that regulate light signaling, rather than endogenous rhythms. Searching for such alleles was the goal of this study.

A cluster analysis identified Lipowiec (Lip-0) as belonging to a group of accessions that showed a late peak of *GI::LUC* expression under LDs (Fig. 1*C* and *SI Appendix*, Tables S3 and S4). Lip-0 *GI::LUC* was crossed to Columbia (Col-0), and extensive phenotyping of the Col-0 X Lip-0 F2 population in different photoperiods confirmed that maximum variability of *GI* peak time was observed in LDs of 16 h (*SI Appendix*, Fig. S3*A*). The F2 population (135 individuals) and subsequently selected F3, F4,

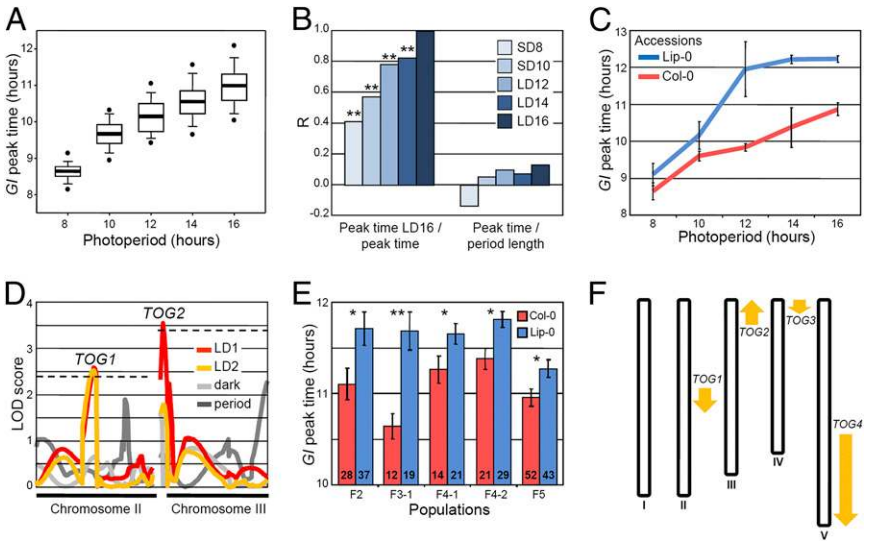

Fig. 1. Natural variation and genetic basis of the timing of *GI* expression during day/night cycles. (*A*) Box plots representing the variation and average (horizontal bars) of *GI* peak time of expression in 77 accessions. (*B*) Correlations between *GI* peak time measured in LDs of 16 h, with *GI* peak time measured in other photoperiods, and between *GI* peak time and period length (DD) measured after entrainment in the same photoperiod. The Pearson correlation coefficient (R) indicates the strength of the correlations, with 1 and −1 indicating perfect positive and negative correlations, respectively. $^{**}P \leq 0.01$. (*C*) *GI* peak time in Col-0 and Lip-0 accessions (mean ± SD of two biological replicates). (*D*) QTL mapping in Col-0 × Lip-0 *GI::LUC* F2 progenies. QTLs were detected for *GI* peak time in two consecutive LDs of 16 h (LD1 and LD2), for *GI* peak time in the first day in darkness after the shift to constant conditions (dark), and for period length in constant darkness (DD). Dashed lines represent LOD thresholds. (*E*) Allelic effect of the *TOG1* QTL in F2, F3, F4, and F5 progenies that were Col-0 or Lip-0 homozygous at *TOG1*. Seedlings were grown in LDs of 16 h. The populations are described in *SI Appendix*, Fig. S4*A* (mean ± SEM; *n* is indicated inside the bars; $^{*}P \leq 0.05$, $^{**}P \leq 0.01$ with a two-tailed Student *t* test). (*F*) Location of the *TOG* QTLs. Upward and downward arrows indicate that the Lip-0 allele advances or delays *GI* peak time, respectively.

and F5 families were used to detect and confirm four *TIMING OF GI* (*TOG*) quantitative trait loci (QTL) of moderate effect that precisely regulated the timing of *GI* expression during the LD 16-h cycle but had no significant effect on period length or on *GI* peak time in darkness (Fig. 1 *D–F* and *SI Appendix*, Figs. S3 and S4 and Table S5). The size and direction of the *TOG* effects were consistent with the phenotype of the Lip-0 parent. Allelic variation at the *TOGs* modified the timing of *GI* expression by ∼30 min, and the Lip-0 alleles of all *TOGs* except one (*TOG2*) delayed *GI* peak time (Fig. 1*F* and *SI Appendix*, Fig. S4). Together with the confirmation of the *TOGs* in near isogenic lines (NILs), these data collectively demonstrate the existence of natural alleles of moderate effect that precisely regulate the timing of *GI* expression within LD day/night cycles (*SI Appendix*, Fig. S5). Previous studies had reported natural variation of daily transcriptional rhythms in the range of hours (14, 17), but our experiments reveal that natural alleles can cause significant variation of a higher level of precision.

The Waveform of *GI* Expression Is Regulated by Light Signaling During LD Cycles. The timing of *GI* expression is influenced by light signaling (*SI Appendix*, Fig. S2*A*), and the related mechanism might explain part of the *GI* peak time variation observed between accessions in LDs. Consistent with this idea, the gene encoding the red light photoreceptor PHYTOCHROME B (PHYB) was present in the *TOG1* region and was a candidate for this QTL. The Lip-0 allele of *PHYB* contains a deletion in the N-terminal part of the protein that is associated with longer hypocotyls and reduced PHYB activity (37) (*SI Appendix*, Fig. S6). Light signaling was previously shown to regulate *GI* (38, 39), but how changes in PHYB activity could modify the timing of *GI* expression in LD day/night cycles was not known (35, 40).

Detailed analysis of *GI* expression in *phyB* mutants revealed that PHYB activity shapes the *GI* waveform by mediating light signals that activate *GI* transcription in the evening of a LD (Fig. 2 and *SI Appendix*, Figs. S7–S9 and *SI Discussion*). On the basis of the results of a mathematical modeling study in which rapid responses to light were predicted to modulate the phase of circadian outputs (36), we first tested how *GI* expression responded to 30 min white or red light pulses applied in darkness after entrainment in LDs. The light pulses triggered an immediate response of *GI::LUC* that was maximal in the evening of the subjective day and that was significantly reduced in the *phyB-9* mutant (Fig. 2 *A* and *B* and *SI Appendix*, Fig. S8 *A* and *B*). During LD cycles, substitution of white light by darkness in the evening suppressed the evening peak of *GI::LUC*, whereas substitution by red light was sufficient for full activation of *GI* (*SI Appendix*, Fig. S8*C*). Importantly, reduced activation of *GI* expression in *phyB* mutants was accompanied by a rightward shift of the *GI* waveform (negative skewness) and by a delay of *GI* peak time that was consistent with *TOG1* Lip-0 delaying *GI::LUC* expression (Fig. 2 *C–E* and *SI Appendix*, Figs. S7 *A*, *D*, *F* and S8 *D* and *E*). This effect was specific to LDs of 16 h (*SI Appendix*, Figs. S7 *B* and *C* and S10) and had been reported for rhythms of cytosolic Ca^{2+} (36), but was not detected with a circadian marker that was not regulated by light (Fig. 2*E*). These results provide a mechanistic understanding of how light signaling shapes the waveform of *GI* expression in LDs and support a role for rapid responses to light in determining the phase of circadian outputs (36). The circadian clock is implicated in this mechanism not by modifying endogenous rhythms in DD or in LL but by gating (constraining) light activation of *GI* transcription in the evening (Fig. 2*E* and *SI Appendix*, Figs. S6 *C* and *D* and S7*E* and *SI Discussion*).

We then asked whether natural *TOG* alleles regulate *GI* through the same mechanism. Similar to the *phyB-9* mutation, the less active *TOG1* Lip-0 allele reduced *GI::LUC* evening expression levels in F2 progenies (*SI Appendix*, Fig. S11 *A–C*). *TOG1* Lip-0 also reduced *GI::LUC* expression in segregating populations generated by crossing *phyB-9* with two NILs that carried the *TOG1* Col-0 or Lip-0 alleles (*SI Appendix*, Fig. S11*C*). The effects of the different allelic combinations obtained in these populations were consistent with *PHYB* being the gene underlying *TOG1*. We next combined Lip-0 alleles of *TOG1-4* in the Col-0 background and created a population of 12 NILs that we used to more generally address how the *TOGs* were regulating *GI* (*SI Appendix*, Fig. S12*A*). Again similar to the analysis of *phyB* mutants, *GI* peak time significantly and negatively correlated with maximum *GI* expression levels in the NIL population grown in LDs of 16 h, and changes in peak time occurred at least partly independent of circadian rhythms in DD or in LL (*SI Appendix*, Fig. S12 *B* and *C*, Table S7, and *SI Discussion*). Thus, the detailed description of *GI* expression patterns in various populations supports a role for the *TOGs* in mediating a direct effect of light on the *GI* promoter through a mechanism that involves PHYB activity.

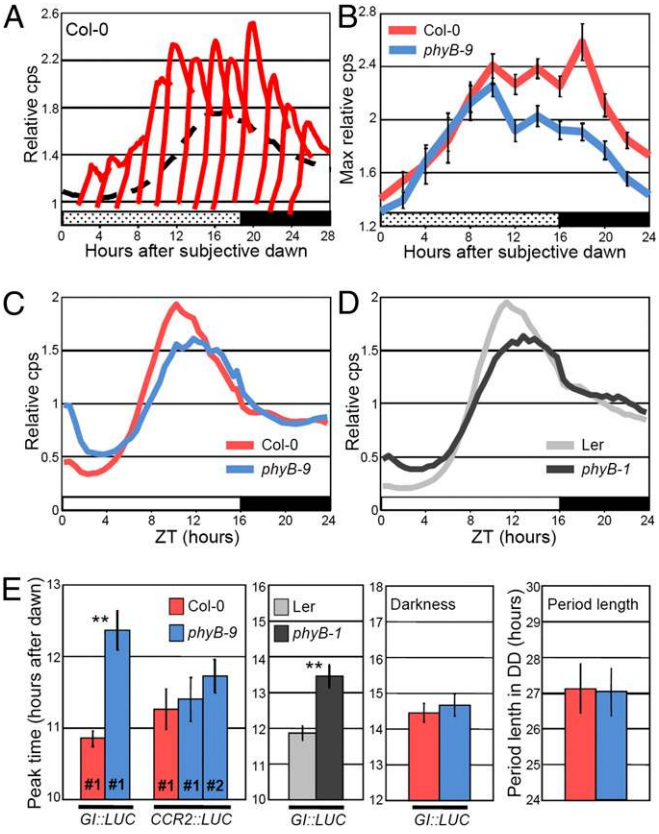

Fig. 2. Light signaling defines the temporal waveform of *GI* expression during LDs. In all experiments, plants were entrained during 9 d in LDs of 16 h and *GI::LUC* expression was monitored on day 10 unless otherwise stated. (*A* and *B*) Col-0 and *phyB-9* plants were entrained in LDs of 16 h, transferred to DD, and exposed to 30-min red light pulses of 60 $\mu mol \cdot m^{-2} \cdot s^{-1}$ applied every 2 h during the first subjective day. The response of *GI::LUC* expression to each pulse (*A*) is expressed relative to the expression level (cps, counts per second) measured before the pulse. The dashed line represents the nontreated control in DD (not to scale). Maximum relative luminescence after each pulse was plotted in (*B*). (*C* and *D*) Waveform of *GI::LUC* expression in (*C*) Col-0 and *phyB-9* and in (*D*) Ler and *phyB-1* in LDs of 16 h. (*E*) Peak time of *GI::LUC* expression in LDs of 16 h in Col-0 and *phyB-9*, of *CCR2::LUC* expression in Col-0, and in two independent *phyB-9* transgenic lines, of *GI::LUC* expression in the Ler and *phyB-1* background, of *GI::LUC* expression measured in the first day in DD and of period length measured in DD. Confirmation of these results with more transgenic lines is provided in *SI Appendix*, Fig. S7. Mean ± SEM; n = 12–24; $*P \leq 0.05$, $**P \leq 0.01$ with a two-tailed Student t test.

Precise Changes in the Waveform of *GI* Expression Are Sufficient to Alter a Downstream Phenotype. The *TOGs* cause precise changes in the daily pattern of *GI* expression, but it remained to be

determined whether changes of such magnitude were biologically relevant and could affect overt phenotypes. We used hypocotyl growth as a phenotypic output of GI activity and tested whether alterations of this trait could be a result of precise changes in the *GI* expression waveform. A major advantage of using growth as a trait was that it can be precisely quantified in conditions directly comparable to the ones used for the *GI::LUC* activity assays. GI represses growth of the hypocotyl (27), but how GI function contributes to the molecular network that regulates growth in day/night conditions, and particularly in LDs, was not known.

GI acts in the hypocotyl growth repression pathway activated by PHYB (27), which, according to our results, could at least partially be explained by PHYB-mediated activation of *GI* expression. GI is also known to reduce mRNA levels of the transcription factor *PHYTOCHROME INTERACTING FACTOR 4* (*PIF4*) during the night when PIF4 contributes to the promotion of growth (41–43). Loss of *GI* function in the Col-0 background also enhanced *PIF4* expression in our conditions, and the long hypocotyl phenotype of *gi-2* required PIF4 activity (Fig. 3 *A* and *B*). We further found that GI and PHYB act synergistically to inhibit growth and repress *PIF4* during the night. Enhanced hypocotyl growth of *phyB-9 gi-2* compared with *phyB-9* required functionally active PIF4 and was associated with increased *PIF4* expression levels (Fig. 3 *A* and *B*). As PHYB also promotes degradation of PIF4 at dawn (41), the synergy between GI and PHYB probably acts at both the transcriptional and posttranscriptional levels (Fig. 3*C*).

In the NILs, growth was affected through the same mechanism. *GI::LUC* expression levels and peak time, but not period length, strongly correlated with hypocotyl length and *PIF4* mRNA levels measured in LDs of 16 h (Fig. 3 *D–F*). The correlations between *GI* expression levels and hypocotyl length or *PIF4* mRNA were negative, which was consistent with GI being a repressor of growth. The data also confirmed the model for the regulation of *GI* transcription by light via the *TOGs*. If the *TOGs* regulate *GI* expression in the evening, phenotypic changes downstream of GI in the NILs should be induced by variations of *GI* expression at this time. As anticipated, the correlations between *GI::LUC* expression levels and *PIF4* mRNA or growth were strongest during the second part of the day, which was also the time when the differences in *GI::LUC* activity between NILs were more pronounced (Fig. 4 *A* and *B*). Thus, natural *TOG* alleles regulate *PIF4* expression and growth in LDs, at least partly by modifying the waveform of *GI* transcription in the evening and in a way that would be enhanced by changes in PHYB activity (Fig. 4*C* and *SI Appendix*, *SI Discussion*).

These data additionally provide novel insights on the function of GI and on the growth regulation model. First, they show that circadian-gated expression of *GI* in the evening contributes to the temporal regulation of hypocotyl length. Second, they reveal how light signaling regulates *PIF4* expression during day/night cycles. The underlying mechanism might involve coexpression and functional interactions of GI with components of the EVENING COMPLEX (EC), a protein complex that directly represses *PIF4* (42–44) (Fig. 4*C*). Interestingly, we detected no significant relationship between *GI* expression and flowering in the NILs, despite an important function of GI being the promotion of flowering through the regulation of *CONSTANS* (*CO*) (45, 46). GI regulates diverse traits through distinct molecular pathways (47–49), and it is possible that these pathways are not all equally sensitive to precise changes in *GI* expression. GI-mediated promotion of flowering might be more robust than growth to small perturbations of *GI* expression and function, an idea supported by a previous study in which an induced mutation of *GI* altered growth but not GI-dependent promotion of *CO* (48). A similar scenario could explain why precise changes in *GI* expression do not alter flowering time in the NILs but do affect growth through the regulation of *PIF4* transcription.

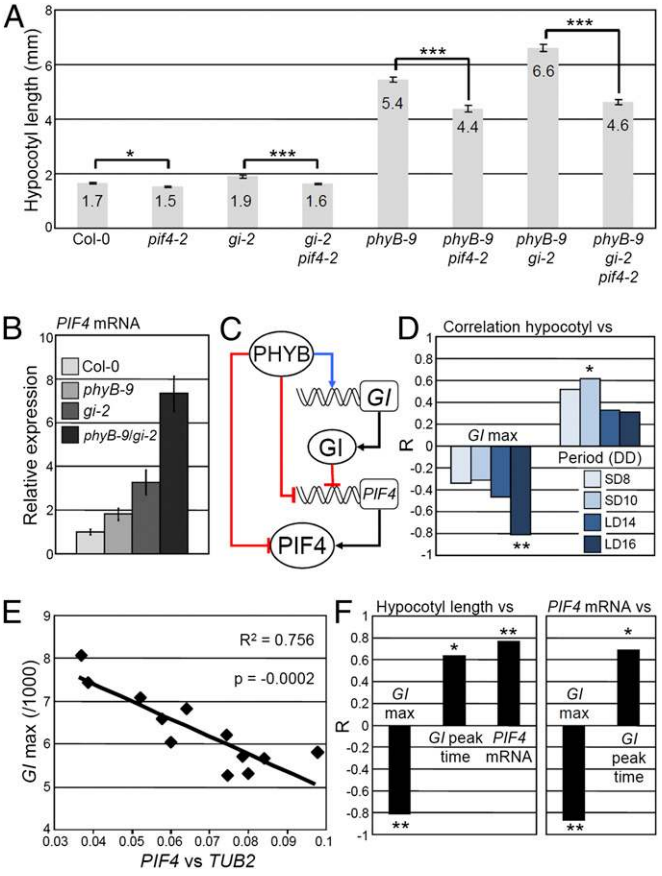

Fig. 3. Precise changes in *GI* expression modify *PIF4* expression and growth. (*A*) Hypocotyl length and (*B*) *PIF4* mRNA levels at zeitgeber time (ZT) 20 h, quantified by quantitative RT-PCR (qRT-PCR) in LDs of 16 h in the indicated mutant backgrounds. (*C*) Working model for how PHYB and GI interact to regulate growth. Red lines indicate repression, blue lines activation, and black lines translation. Rectangles and circles represent genes and proteins, respectively. (*D*) Correlation of hypocotyl length of the NILs grown in LDs of 16 h with *GI::LUC* expression level at peak time (*GI* max) and period length in DD after entrainment in four photoperiods. (*E*) Correlation between *GI::LUC* expression level at peak time (*GI* max) and *PIF4* mRNA levels quantified by qRT-PCR in the NILs entrained in LDs of 16 h and sampled at ZT 20 h. (*F*) Correlation among growth, *GI::LUC* expression level at peak time (*GI* max), *GI* peak time, and *PIF4* mRNA levels at ZT 20 h. The Pearson correlation coefficient (R) indicates the strength of the correlations, with 1 and −1 indicating perfect positive and negative correlations, respectively. $*P \leq 0.05$, $**P \leq 0.01$, and $***P \leq 0.001$, with (*A*) a two-tailed Student *t* test or (*D* and *F*) the Pearson test. The correlations were also tested with the Spearman test and yielded similar results.

Conclusions and Perspectives

Collectively, our findings provide a paradigm for how natural alleles cause phenotypic diversity by precisely altering daily waveforms of gene expression. We also show that natural variation in temporal rhythms of expression during the day can be determined by changes in sensitivity to input signals, and not only by changes in circadian rhythms. The LD-specific mechanism of *GI* regulation we describe is part of a more general external coincidence model for the global control of phase in day/night conditions (36). The model predicts that the evening phase of processes dual-regulated by light and by the circadian clock adjusts to seasonal changes by responding predominantly to rapid light inputs. Natural alleles implicated in the perception of input signals that influence rhythms might explain why period length and phase generally do not correlate in *Arabidopsis* accessions. Such natural alleles could confer an advantage by

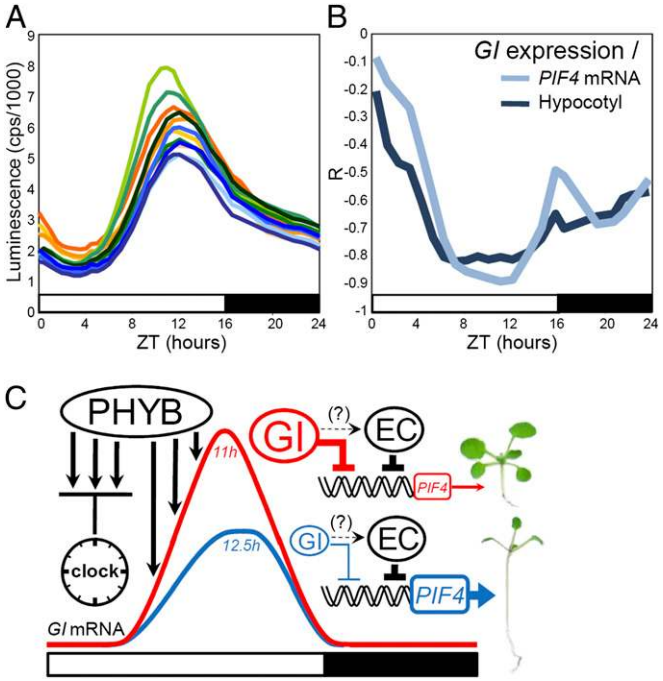

Fig. 4. GI regulates growth by acting predominantly in the evening. (*A*) Waveforms of *GI::LUC* expression in the NILs in LDs of 16 h. (*B*) Pearson coefficient (R) of correlations between *GI::LUC* expression at different times of the day with hypocotyl length and *PIF4* mRNA levels at ZT 20 h in the NILs. R indicates the strength of the correlations, with 1 and −1 indicating perfect positive and negative correlations, respectively. (*C*) A model for the regulation of *GI* expression by natural alleles during the day, and how this affects *PIF4* expression and growth. Light signaling mediated by PHYB is repressed by the circadian clock in the morning of a long day. Clock repression is released later during the day, so that light activates *GI* expression until it reaches its peak in the evening. GI then contributes to the repression of *PIF4* early in the night, so that growth is less efficiently promoted. Weak PHYB alleles cause less GI accumulation (blue line), more *PIF4* transcription, and more growth. GI could hypothetically regulate *PIF4* transcription by interacting with the EC, as represented by the dashed lines. Blue and red lines represent the *GI* waveform when influenced by weak or strong *PHYB* alleles, respectively. Numbers in italics indicate representative *GI* peak times.

optimizing the activity of temporally regulated processes while avoiding the pleiotropic effects associated with severe disruptions of the circadian system (5).

Rhythms of gene expression were analyzed within day/night cycles, at high temporal resolution, and in a population of natural accessions large enough to estimate the range of variation that exists at the intraspecies level. We then revealed the precision with which natural alleles modify daily expression patterns and demonstrated that these modifications have detectable effects on growth, a complex quantitative trait known to be under the control of many small effect loci (50, 51). Theoretical models predict that loci of small effect are a major source of phenotypic variation (52), but understanding how these loci modify phenotypes has been limited by the technical difficulties of their detection and validation. The exploitation of marker gene technology such as luciferase to identify alleles with small phenotypic effects may represent a general approach to uncovering such variation.

Methods

Plant Material and Growth Conditions. The 77 accessions used in this work were a donation from Thomas Altmann, Leibniz Institute of Plant Genetics and Crop Plant Research (IPK), Gatersleben, Germany, and a subset of these accessions was previously described elsewhere (53). The *phyB-9* and *gi-2* mutant alleles also were described previously (54, 55). To obtain the *GI::LUC* transgene, a 2,513-bp fragment of the *GI* promoter was amplified, using primer 5′-attB1-accagcatatctctaatcag-3′ and primer 5′-attB2-accgaaactaaaccccaac-3′, and recombined with the pGWLuc vector (GeneBank: AM295157). The *GI::LUC* transgene was inserted into *Arabidopsis* by Agrobacterium-mediated transformation (56). Col-0 and *phyB-9 GI::LUC* lines 2 and 3 were obtained after transformation with a vector containing 2,755 bp of the *GI* promoter and were described elsewhere (35). Transgenic lines were made homozygous before use. The first 39 accessions were scored using at least two transgenic lines per accession. A significant contribution of the genotype (accessions) to variations of *GI::LUC* expression was detected in this data set (*SI Appendix*, Table S2). Only one line per accession was subsequently used to reduce the workload. Seedlings were grown in different photoperiods at 22 °C under 100 $\mu mol \cdot m^{-2} \cdot s^{-1}$ fluorescent white light (Philips TL741), or in a Percival growth chamber equipped with E-30LED for monochromatic light experiments (Percival).

Bioluminescence Imaging. Plants were entrained for 9 d in different photoperiods and light conditions, and measurements were started on day 10. For experiments performed in white light, seedlings were transferred to 96-well black optiplates (Perkin-Elmer Life Sciences) containing Murashige and Skoog medium with 2% (mass/vol) sucrose and 20 μL D-luciferin (5 mM). Luminescence of individual seedlings was monitored in a TopCount Microplate Scintillation Counter (Perkin-Elmer) by manual feeding, which allowed the study of *GI* expression in white light conditions that contained the whole spectrum of wavelengths. In constant darkness (DD) conditions, feeding of the plates to the TopCount was automatic. LUC activity in monochromatic red light was monitored with a CCD camera in 24-well plates containing approximately 10 seedlings of the same genotype and supplied with 150 μL of 10 mM Luciferin. The resolution of the assays was 30 min. The images generated by the CCD camera were analyzed with Metamorph (Molecular Devices). Rhythms of *GI::LUC* expression during day/night cycles or in constant conditions were analyzed with BRASS (www.amillar.org).

QTL Detection and Statistical Analyses. The QTLs were detected in 135 F2 progenies scored for *GI::LUC* expression and genotyped by Sequenom Inc. Linkage maps were created using JoinMap 4 (Kyazma B.V.), and QTL analysis was performed with MapQTL 5 (Kyazma B.V.), using the multiple QTL mapping (MQM) procedure. A thousand permutations were used to determine chromosome-specific logarithm of odds (LOD) thresholds. Markers used as cofactors were chosen by backward selection. More detailed information on the phenotyping and genotyping procedures and on the QTL validation in segregating populations and in the NILs is provided in *SI Appendix, SI Methods*. Hierarchical clustering was performed using Cluster version 3. The raw data were mean centered and normalized across the different day lengths. Clustering was performed with an uncentered correlation matrix and average linkage clustering. Self-organizing maps were generated before hierarchical clustering to determine the best orientation of the tree nodes. The resulting trees were displayed using Treeview version 3. All other statistical analyses were performed with SigmaStat version 3 or R.

Hypocotyl Measurements. Hypocotyl length of the seedlings grown under different photoperiods and light conditions was measured after 9 days so the data would be directly comparable to the luciferase data. A high-resolution photograph of the seedlings was taken with a digital camera, and hypocotyl length was measured with Image J (National Institutes of Health). In all experiments, ∼20–30 seedlings per genotype were analyzed. Hypocotyl data for the NILs were obtained from five independent biological replicates performed in each of the four photoperiods tested (4,632 seedlings total).

Quantification of mRNA Expression. RNA was isolated from 10-day-old seedlings, using the RNeasy Plant Mini kit (Qiagen), following the recommendations of the manufacturer. Genomic DNA was removed with the DNA-free kit (Ambion). For cDNA synthesis, 1 μg total RNA was primed using the oligodT primer and reverse transcribed with the SuperScript II kit (Invitrogen). The PCR mix was composed of 3 μL diluted cDNA and 7 μL iQ SYBR Green Supermix (Biorad). The thermocycles used for amplification were 3 min at 95 °C, followed by 40 cycles of 10 s at 95 °C, 10 s at 60 °C, and 10 s at 72 °C. *TUB2* (At5g62690) and *IPP2* (At3g02780) were used as housekeeping genes to normalize the expression data and yielded similar results. Primer sequences are provided in *SI Appendix*, Table S8.

ACKNOWLEDGMENTS. We thank M. Koornneef, S. Davis, J. Jimenez Gomez, and F. Fornara for critical reading of the manuscript. We also thank E. de Ansorena for excellent technical assistance. This work was supported by a Marie Curie fellowship from the European Commission (A.d.M.) and by a core funding of the Max Planck Society (G.C.).

1. de Montaigu A, Tóth R, Coupland G (2010) Plant development goes like clockwork. *Trends Genet* 26(7):296–306.
2. Wang W, et al. (2011) Timing of plant immune responses by a central circadian regulator. *Nature* 470(7332):110–114.
3. Harmer SL (2009) The circadian system in higher plants. *Annu Rev Plant Biol* 60: 357–377.
4. Michael TP, et al. (2003) Enhanced fitness conferred by naturally occurring variation in the circadian clock. *Science* 302(5647):1049–1053.
5. Dodd AN, et al. (2005) Plant circadian clocks increase photosynthesis, growth, survival, and competitive advantage. *Science* 309(5734):630–633.
6. Somers DE, Devlin PF, Kay SA (1998) Phytochromes and cryptochromes in the entrainment of the Arabidopsis circadian clock. *Science* 282(5393):1488–1490.
7. Michael TP, Salome PA, McClung CR (2003) Two Arabidopsis circadian oscillators can be distinguished by differential temperature sensitivity. *Proc Natl Acad Sci USA* 100(11):6878–6883.
8. Salomé PA, To JP, Kieber JJ, McClung CR (2006) Arabidopsis response regulators ARR3 and ARR4 play cytokinin-independent roles in the control of circadian period. *Plant Cell* 18(1):55–69.
9. Millar AJ, Kay SA (1996) Integration of circadian and phototransduction pathways in the network controlling CAB gene transcription in Arabidopsis. *Proc Natl Acad Sci USA* 93(26):15491–15496.
10. Fowler SG, Cook D, Thomashow MF (2005) Low temperature induction of Arabidopsis CBF1, 2, and 3 is gated by the circadian clock. *Plant Physiol* 137(3):961–968.
11. Li G, et al. (2011) Coordinated transcriptional regulation underlying the circadian clock in Arabidopsis. *Nat Cell Biol* 13(5):616–622.
12. Hayama R, Yokoi S, Tamaki S, Yano M, Shimamoto K (2003) Adaptation of photoperiodic control pathways produces short-day flowering in rice. *Nature* 422(6933): 719–722.
13. Turner A, Beales J, Faure S, Dunford RP, Laurie DA (2005) The pseudo-response regulator Ppd-H1 provides adaptation to photoperiod in barley. *Science* 310(5750): 1031–1034.
14. Böhlenius H, et al. (2006) CO/FT regulatory module controls timing of flowering and seasonal growth cessation in trees. *Science* 312(5776):1040–1043.
15. Izawa T, et al. (2011) Os-GIGANTEA confers robust diurnal rhythms on the global transcriptome of rice in the field. *Plant Cell* 23(5):1741–1755.
16. Kloosterman B, et al. (2013) Naturally occurring allele diversity allows potato cultivation in northern latitudes. *Nature* 495(7440):246–250.
17. Slotte T, Holm K, McIntyre LM, Lagercrantz U, Lascoux M (2007) Differential expression of genes important for adaptation in Capsella bursa-pastoris (Brassicaceae). *Plant Physiol* 145(1):160–173.
18. Swarup K, et al. (1999) Natural allelic variation identifies new genes in the Arabidopsis circadian system. *Plant J* 20(1):67–77.
19. Edwards KD, Lynn JR, Gyula P, Nagy F, Millar AJ (2005) Natural allelic variation in the temperature-compensation mechanisms of the Arabidopsis thaliana circadian clock. *Genetics* 170(1):387–400.
20. Boikoglou E, et al. (2011) Environmental memory from a circadian oscillator: The Arabidopsis thaliana clock differentially integrates perception of photic vs. thermal entrainment. *Genetics* 189(2):655–664.
21. Anwer MU, et al. (2014) Natural variation reveals that intracellular distribution of ELF3 protein is associated with function in the circadian clock. *eLife* 3:3.
22. Darrah C, et al. (2006) Analysis of phase of LUCIFERASE expression reveals novel circadian quantitative trait loci in Arabidopsis. *Plant Physiol* 140(4):1464–1474.
23. Eimert K, Wang SM, Lue WI, Chen J (1995) Monogenic Recessive Mutations Causing Both Late Floral Initiation and Excess Starch Accumulation in Arabidopsis. *Plant Cell* 7(10):1703–1712.
24. Kurepa J, Smalle J, Van Montagu M, Inzé D (1998) Oxidative stress tolerance and longevity in Arabidopsis: The late-flowering mutant gigantea is tolerant to paraquat. *Plant J* 14(6):759–764.
25. Park DH, et al. (1999) Control of circadian rhythms and photoperiodic flowering by the Arabidopsis GIGANTEA gene. *Science* 285(5433):1579–1582.
26. Fowler S, et al. (1999) GIGANTEA: A circadian clock-controlled gene that regulates photoperiodic flowering in Arabidopsis and encodes a protein with several possible membrane-spanning domains. *EMBO J* 18(17):4679–4688.
27. Huq E, Tepperman JM, Quail PH (2000) GIGANTEA is a nuclear protein involved in phytochrome signaling in Arabidopsis. *Proc Natl Acad Sci USA* 97(17):9789–9794.
28. Dalchau N, et al. (2011) The circadian oscillator gene GIGANTEA mediates a long-term response of the Arabidopsis thaliana circadian clock to sucrose. *Proc Natl Acad Sci USA* 108(12):5104–5109.
29. Kim WY, et al. (2013) Release of SOS2 kinase from sequestration with GIGANTEA determines salt tolerance in Arabidopsis. *Nat Commun* 4:1352.
30. Dunford RP, Griffiths S, Christodoulou V, Laurie DA (2005) Characterisation of a barley (Hordeum vulgare L.) homologue of the Arabidopsis flowering time regulator GIGANTEA. *Theor Appl Genet* 110(5):925–931.
31. Zhao XY, Liu MS, Li JR, Guan CM, Zhang XS (2005) The wheat TaGI1, involved in photoperiodic flowering, encodes an Arabidopsis GI ortholog. *Plant Mol Biol* 58(1): 53–64.
32. Hecht V, et al. (2007) Pea LATE BLOOMER1 is a GIGANTEA ortholog with roles in photoperiodic flowering, deetiolation, and transcriptional regulation of circadian clock gene homologs. *Plant Physiol* 144(2):648–661.
33. Onai K, et al. (2004) Large-scale screening of Arabidopsis circadian clock mutants by a high-throughput real-time bioluminescence monitoring system. *Plant J* 40(1):1–11.
34. Ding Z, Millar AJ, Davis AM, Davis SJ (2007) TIME FOR COFFEE encodes a nuclear regulator in the Arabidopsis thaliana circadian clock. *Plant Cell* 19(5):1522–1536.
35. Palágyi A, et al. (2010) Functional analysis of amino-terminal domains of the photoreceptor phytochrome B. *Plant Physiol* 153(4):1834–1845.
36. Dalchau N, et al. (2010) Correct biological timing in Arabidopsis requires multiple light-signaling pathways. *Proc Natl Acad Sci USA* 107(29):13171–13176.
37. Filiault DL, et al. (2008) Amino acid polymorphisms in Arabidopsis phytochrome B cause differential responses to light. *Proc Natl Acad Sci USA* 105(8):3157–3162.
38. Locke JC, et al. (2005) Extension of a genetic network model by iterative experimentation and mathematical analysis. *Mol Syst Biol* 1:2005.0013.
39. Paltiel J, Amin R, Gover A, Ori N, Samach A (2006) Novel roles for GIGANTEA revealed under environmental conditions that modify its expression in Arabidopsis and Medicago truncatula. *Planta* 224(6):1255–1268.
40. Salomé PA, et al. (2002) The out of phase 1 mutant defines a role for PHYB in circadian phase control in Arabidopsis. *Plant Physiol* 129(4):1674–1685.
41. Nozue K, et al. (2007) Rhythmic growth explained by coincidence between internal and external cues. *Nature* 448(7151):358–361.
42. Nusinow DA, et al. (2011) The ELF4-ELF3-LUX complex links the circadian clock to diurnal control of hypocotyl growth. *Nature* 475(7356):398–402.
43. Kim Y, et al. (2012) GIGANTEA and EARLY FLOWERING 4 in Arabidopsis exhibit differential phase-specific genetic influences over a diurnal cycle. *Mol Plant* 5(3): 678–687.
44. Kim Y, et al. (2013) ELF4 regulates GIGANTEA chromatin access through subnuclear sequestration. *Cell Reports* 3(3):671–677.
45. Sawa M, Nusinow DA, Kay SA, Imaizumi T (2007) FKF1 and GIGANTEA complex formation is required for day-length measurement in Arabidopsis. *Science* 318(5848): 261–265.
46. Fornara F, et al. (2009) Arabidopsis DOF transcription factors act redundantly to reduce CONSTANS expression and are essential for a photoperiodic flowering response. *Dev Cell* 17(1):75–86.
47. Mizoguchi T, et al. (2005) Distinct roles of GIGANTEA in promoting flowering and regulating circadian rhythms in Arabidopsis. *Plant Cell* 17(8):2255–2270.
48. Martin-Tryon EL, Kreps JA, Harmer SL (2007) GIGANTEA acts in blue light signaling and has biochemically separable roles in circadian clock and flowering time regulation. *Plant Physiol* 143(1):473–486.
49. Oliverio KA, et al. (2007) GIGANTEA regulates phytochrome A-mediated photomorphogenesis independently of its role in the circadian clock. *Plant Physiol* 144(1): 495–502.
50. Kroymann J, Mitchell-Olds T (2005) Epistasis and balanced polymorphism influencing complex trait variation. *Nature* 435(7038):95–98.
51. Joseph B, et al. (2013) Hierarchical nuclear and cytoplasmic genetic architectures for plant growth and defense within Arabidopsis. *Plant Cell* 25(6):1929–1945.
52. Rockman MV (2012) The QTN program and the alleles that matter for evolution: All that's gold does not glitter. *Evolution* 66(1):1–17.
53. Narang RA, Bruene A, Altmann T (2000) Analysis of phosphate acquisition efficiency in different Arabidopsis accessions. *Plant Physiol* 124(4):1786–1799.
54. Rédei GP (1962) Supervital Mutants of Arabidopsis. *Genetics* 47(4):443–460.
55. Reed JW, Nagpal P, Poole DS, Furuya M, Chory J (1993) Mutations in the gene for the red/far-red light receptor phytochrome B alter cell elongation and physiological responses throughout Arabidopsis development. *Plant Cell* 5(2):147–157.
56. Clough SJ, Bent AF (1998) Floral dip: A simplified method for Agrobacterium-mediated transformation of Arabidopsis thaliana. *Plant J* 16(6):735–743.

Natural diversity in daily rhythms of gene expression contributes to phenotypic variation

Supporting Methods, Discussion, Figures and Tables

Amaury de Montaigu, Antonis Giakountis, Matthew Rubin, Réka Tóth, Frederic Cremer, Vladislava Sokolova, Aimone Porri, Matthieu Reymond, Cynthia Weinig and George Coupland

Corresponding autor:

George Coupland

Max Planck Institute for Plant Breeding Research, Carl von LinneWeg 10, D-50829 Cologne, Germany.

coupland@mpipz.mpg.de

Supporting Methods

Additional information on the phenotyping and genotyping procedures.

Seeds were surface sterilized for 10 minutes in 70 % (vol/vol) ethanol, 5 minutes in 100 % (vol/vol) ethanol and washed three times in sterile water. The seeds were then stratified 3 days at 4°C and plated on MS medium with 2% (m/vol) sucrose. In the case of experiments carried out in monochromatic red light, seeds were left 6 hours in white light to induce germination before being placed in a Percival growth chamber.

F2 individuals from the original mapping population were scored for *GI::LUC* activity and subsequently transferred to soil so that leaf material could be harvested for DNA extraction. Seeds from each individual were collected for analysis of the offspring. DNA was extracted from 100 mg of leaf tissue with the Biosprint robot (Qiagen), following the recommendations of the manufacturer. Genotyping of the F2 and F3 populations was performed by Sequenom inc. using a set of 96 markers that had previously been identified from a pool of 360 polymorphisms.

QTL validation in the F3, F4 and F5 progenies was performed following the same procedure than in the F2. Up to 96 individuals per population were phenotyped, transferred to soil and subsequently genotyped. Genotyping of the segregating regions in F4 and F5 populations was performed with CAPS (Cleaved Amplified Polymorphic Sequences), dCAPS or SSLP (Simple Sequence Length Polymorphism) markers designed based on the polymorphisms identified by Sequenom inc., polymorphism described elsewhere (1), and polymorphism information provided by TAIR (www.arabidopsis.org). Polymorphic regions were PCR amplified, digested with the appropriate restriction enzyme in the case of CAPs and dCAPs, and DNA products were visualized on agarose gels.

Generation of the NILs.

The generation of the NILs was initiated with population F3-1 (Fig. S4). The parent of F3-1 was an F2 plant isolated in the original mapping population and whose genotype is presented in Fig. S4*A*. 63 individuals of population F3-1 were genotyped by Sequenom inc. with the complete 96 marker set. From these data we obtained the parent of population F4-3 that was Col-0 homozygous for most of the genetic background, and that was homozygous Lip-0 or heterozygous at the position of the four *TOG* QTLs (Fig. S4*A*). This extra round of genotyping with the complete 96 marker set also excluded any possible contamination of the population. 192 individuals from population F4-3 were then genotyped with a set of in house markers distributed across the genome and designed based on (1), on the information from Sequenom inc. and on the Arabidopsis database (http://www.arabidopsis.org/). In all the following rounds of genotyping, the genetic background was always checked for Col-0 homozygosity to exclude possible contamination of the populations. The parent of population F5 was isolated from F4-3 as it was almost completely homozygous Col-0 except at the *TOG* loci (Fig. S4*A*). Importantly, all the F3, F4 and F5 families until this point were scored for *GI*::*LUC* expression before genotyping, so that the allelic effect of the *TOG*s was confirmed before introgression of the QTLs. Finally, the parent of the NILs was obtained from the F5 population as it was completely homozygous Col-0 except at the *TOG*s that were Lip-0 homozygous. This individual was backcrossed to Col-0 and a recombination event reduced the size of the *TOG*1 introgression. At this stage all the *TOG*s were heterozygous and individual introgressions of the QTLs could then be obtained in various progenies that we called NILs. We further isolated individuals with combinations of the QTLs in the Col-0 background.

Supporting Discussion

GI peak time is influenced by light signaling and varies at least partly independently of circadian rhythms in Arabidopsis accessions.

In SDs the peak of *GI* expression occurs close to dusk, but in LDs it occurs prior to dusk when plants are still exposed to light (Fig. 1*A* and *C*). We tested whether the peak time of *GI* in SDs was influenced by the onset of darkness at a time when *GI* expression is still rising. We found that in Col-0 plants entrained in SDs of 8 h, an extension of the light period until ZT 16 h delayed the peak of *GI*::*LUC* expression by one hour (Fig. S2*A*). The onset of darkness in SDs therefore causes an abrupt decrease in the transcription of *GI* which results in an apparent peak of transcription close to the time of dusk. This could explain why natural variation of *GI*::*LUC* peak time is limited under SDs, and suggests that a direct effect of light signaling in the evening could contribute to this variation in LDs.

In contrast to peak time, period length measured in DD in the 77 accessions varied to a similar extent after entrainment in all photoperiods tested (Fig. S2*B*). Moreover, period length of plants entrained to 16 h days was equally correlated to that of plants entrained to 14 h or 8 h days (Fig. S2*C*). These results do not support the existence of a mechanism that creates variability of period length specifically in LD photoperiods, as observed for *GI* peak time.

A direct effect of light signaling in the evening alters the waveform of *GI* transcription during LDs.

PHYB regulates the acute response to light of *GI* transcription in the evening (Fig. 2*A* and *B*), and a single 30 min pulse of white or red light during the subjective evening confirmed that PHYB was required for *GI* to fully respond to light (Fig. S8*A* and *B*). After a shift from white light to red light at ZT 8 h in LDs, loss of PHYB activity modified the waveform and delayed the timing of *GI* expression (Fig. S8*D* and *E*). However, after a shift to darkness at the same time of day, the effect of the *phyB-9* mutation on the *GI* waveform was reduced (Fig. S8*D* and *E*). Therefore, the presence of white or red light in the evening of a LD is required for the *phyB-9* mutation to delay *GI* expression. We also studied how changes in circadian rhythms were implicated in the regulation of *GI* peak time during LD conditions. Consistent with previous reports (2), PHYB loss of function in our conditions did not alter the period of *GI::LUC* oscillations in constant DD (Fig. 2*E*) but did lengthen period in constant red light (Fig. S7*E*). Notably, the difference in peak time under red light LDs between Col-0 and *phyB-9* was more than twice the difference in period length detected in red light LL (Fig. S7*D* and *E*), suggesting that the change in period length does not fully account for the change in peak time even in this condition. In our experiments, the effect of PHYB on *GI* was detected in LDs but not in SDs and not in the first day in DD immediately following the LD cycles (Fig. 2*E* and Fig. S7*B* and *C*). Moreover, a second circadian marker, *CCR2::LUC*, which is expressed at a similar time of day to *GI::LUC* was not affected by the *phyB-9* mutation in LDs (Fig. 2*E*). Taken together, the results show that a direct effect of light influences the timing and waveform of *GI* expression in LDs at least partly independently of circadian rhythms.

Alterations of PHYB activity also led to lower absolute expression levels of *GI* in the evening. The *TOG1* Lip-0 allele and the *phyB-9* mutation significantly reduced maximum *GI*::*LUC* expression, generally supporting that PHYB activity promotes *GI* expression in the evening (Fig. S11*B* and *C*). This was confirmed in qRT PCR experiments as evening expression levels of the endogenous *GI* gene was reduced in

phyB-9 and increased in a PHYB overexpressor (Fig. S9*A*). The *phyB-9* mutation also altered *GI* mRNA levels 1 h and 1.5 h after a light pulse as described in Fig. S8*A*, and after a light shift at ZT 8 h as described in Fig. S8*C* (Fig. S9*B*-*D*). *LUC* mRNA behaved similarly to *GI* mRNA which, in addition to the results of the luciferase experiments, confirmed the response to genotype and treatment of the *GI* promoter with two different transcripts (Fig. S9*C*).

Analysis of *GI* expression, circadian rhythms, *PIF4* expression and growth in the NILs

By introgressing combinations of the *TOG* QTLs in the Col-0 genetic background we intended to create a set of individuals that had a similar genetic background but that displayed a range of *GI* peak times and expression levels (Fig. S12*A*). *GI*::*LUC* expression was assayed in four photoperiods and statistical analyses confirmed a significant contribution of the genotypic variation to *GI* peak time and expression levels during LDs (Table S7). Similarly than in the *phyB-9* mutant, *GI* peak time significantly and negatively correlated with *GI*::*LUC* maximum expression in LDs of 16 h but not in SDs (Fig. S12*B*). Importantly, peak time variation in the NILs was not explained by changes in circadian rhythms. First, the contribution of the genotypic variation to variation of period length in DD was weak when significant (Table S7). Second, no significant correlations were detected between *GI* peak time and period length in DD (Fig. S12*B*). Third, period length in constant red light positively correlated with peak time (Pearson test: R=0.695, p=0.015) but as in the *phyB-9* mutant the range of *GI* peak time values was broader than period values (Fig. S12*C*).

GI::*LUC* expression significantly correlated with growth and *PIF4* expression in LDs of 16 h but not in other photoperiods (Fig. 3*D*). Four observations generally supported that the relation between *GI* and *PIF4* expression or growth in the NILs was causal. First, PIF4 activity was required for the long hypocotyl phenotype of *gi-2* (Fig. 3*A*). Second, the analysis of *PIF4* expression in the *gi-2* and *phyB-9 gi-2* mutants demonstrated that GI represses *PIF4* expression in LDs of 16 h (Fig. 3*B*). Third, the correlations of *GI::LUC* expression to hypocotyl length and *PIF4* mRNA in the NILs were negative (Fig. 3*D* and *E*), which is consistent with GI being a repressor of growth and of *PIF4* expression. Fourth, the continuous pattern of the correlations implied that a progressive contribution of reduced *GI* expression levels to increased *PIF4* expression was the scenario that best explained the data (Fig. 3*E*). Changes in PHYB activity in the NILs through allelic variation at *TOG1*, and perhaps at other *TOG*s, could also contribute to the variation of *PIF4* expression by acting synergistically with GI (Fig. 3*C*). The increase in *PIF4* expression, combined with an enhancement of PIF4 stabilization, also due to reduced PHYB activity, could then explain part of the changes in growth (Fig. 4*C*).

Supporting References

1. Berendzen K*, et al.* (2005) A rapid and versatile combined DNA/RNA extraction protocol and its application to the analysis of a novel DNA marker set polymorphic between Arabidopsis thaliana ecotypes Col-0 and Landsberg erecta. *Plant Methods* 1:4.
2. Palagyi A, et al. (2010) Functional analysis of amino-terminal domains of the photoreceptor phytochrome B. *Plant Physiology* 153:1834-1845.
3. Filiault DL, et al. (2008) Amino acid polymorphisms in Arabidopsis phytochrome B cause differential responses to light. *Proc Natl Acad Sci U S A* 105:3157-3162.
4. Johanson U*, et al.* (2000) Molecular analysis of FRIGIDA, a major determinant of natural variation in Arabidopsis flowering time. *Science* 290:344-347.

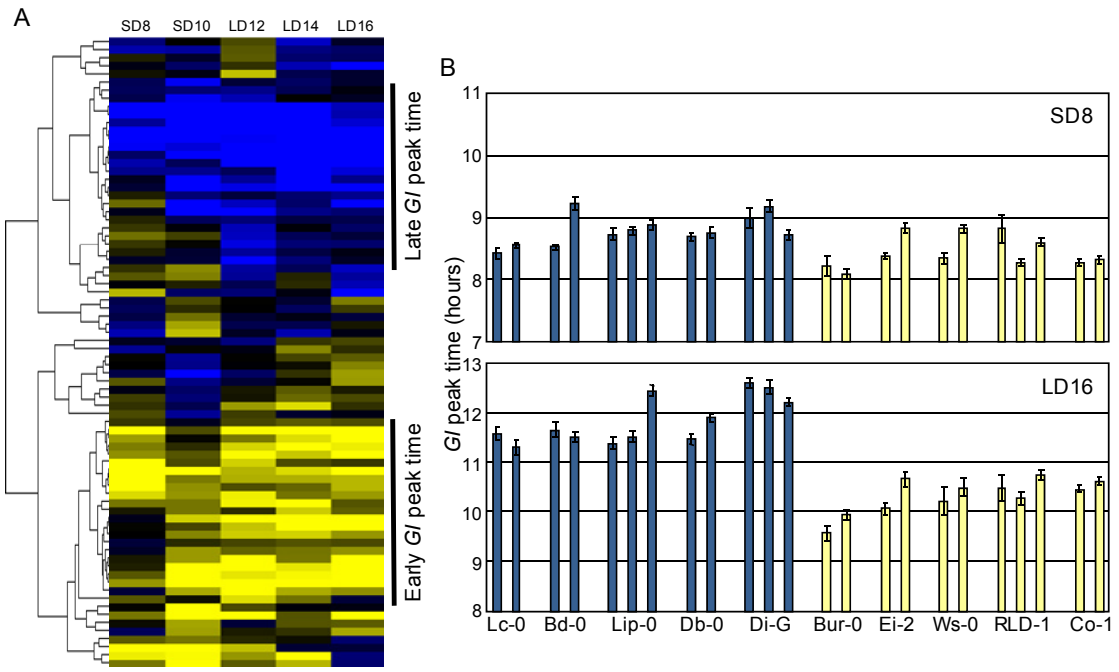

Fig. S1. Natural variation in the timing of *GI* expression in Arabidopsis accessions. (*A*) Hierarchical clustering of *GI* peak times in the accessions. Each row represents an accession and each column represents a photoperiod (SD: short days, LD: long days, number indicates the length of the photoperiod). The data from each photoperiod were mean centered and normalized following the recommended procedure (Cluster version 3). Blue and yellow colors indicate that the *GI* peak time of an accession occurs respectively later or earlier than the average *GI* peak time of all accessions in a photoperiod. Groups of accessions that generally show a late or early *GI* peak time are indicated. (*B*) Example of *GI* peak time data for 10 accessions assayed with multiple transgenic lines. The accessions were selected based on the cluster analysis in *A* and either belong to the group of accessions that generally display a late *GI* peak time (blue bars on the graph), or belong to the group of accessions that generally display an early *GI* peak time (yellow bars on the graph). Results for LDs of 16 h (LD16) and SDs of 8 h (SD8) are shown. These data are a complement to the statistical analysis of Table S2 and illustrate that the insert position did not impede the detection of significant differences in *GI* peak time between accessions. Note that the whole range of variation in LDs 16 h (Fig. 1*A*) is represented in the LD16 panel.

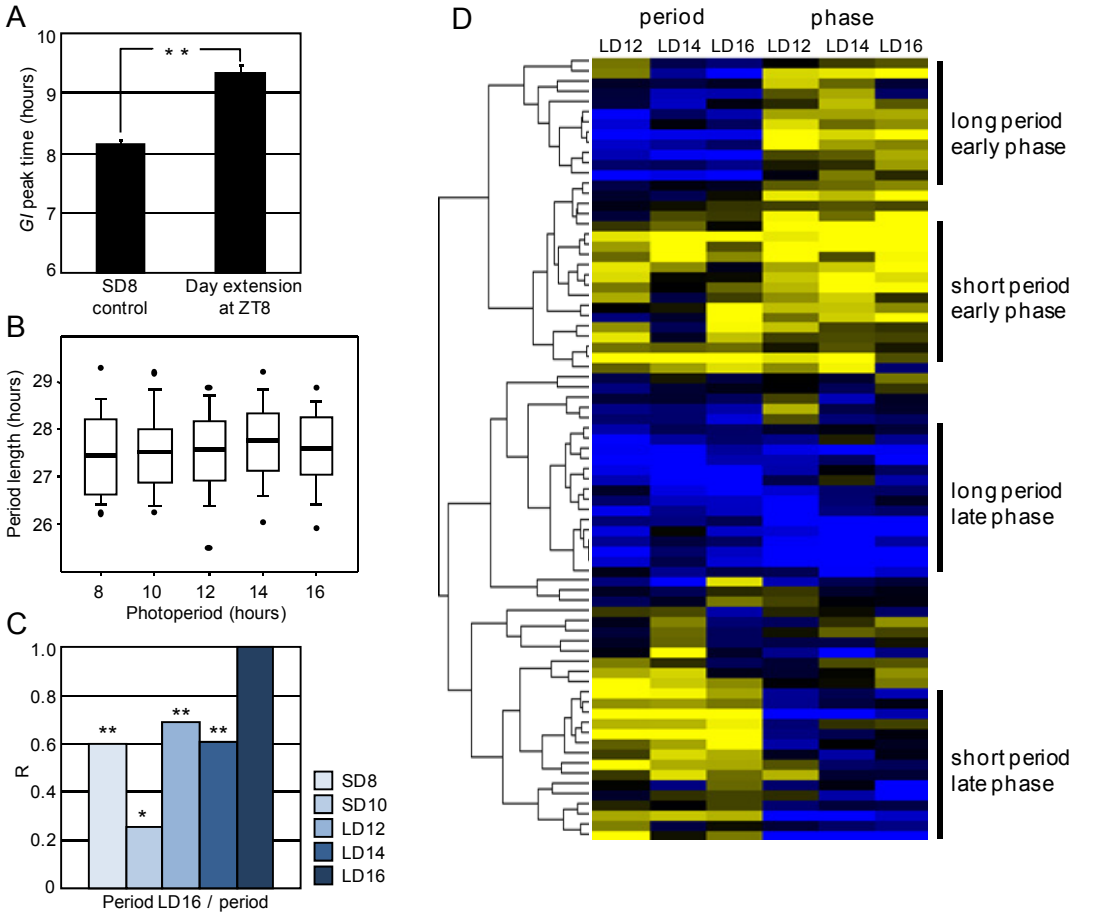

Fig. S2. Light signaling influences the timing of *GI* expression at least partly independently of circadian rhythms. (*A*) *GI* peak time of Col-0 plants entrained in SDs of 8 h and either shifted to darkness or left in white light (day extension) at ZT 8 h on the day of measurement. Error bars represent mean ± s.e.m. **: $p \leq 0.01$ (two tailed Student t-test with $\alpha = 0.05$), $n = 32$. (*B*) Box plots representing the variation of period length in constant darkness (DD) in the 77 accessions after entrainment in 5 photoperiods. Lower and upper limits of the boxes represent 25th and 75th percentile, error bars represent the 10th and 90th percentile and dots represent the 5th and 95th percentile. Horizontal bars represent the mean. (*C*) Correlations between period length in DD after entrainment in LDs of 16 h with period length after entrainment in other photoperiods. The Pearson correlation coefficient (R) indicates the strength of the correlations, 1 and -1 indicating perfect positive and negative correlations respectively. *: $p \leq 0.05$, **: $p \leq 0.01$. (*D*) Hierarchical clustering of *GI* peak time and period length in the accessions. The data from each photoperiod were mean centered and normalized following the recommended procedure (Cluster version 3), and were presented as in Fig. S1*A*. This analysis highlights the existence of two groups of accessions for which period length and phase correlate, and two groups for which they do not.

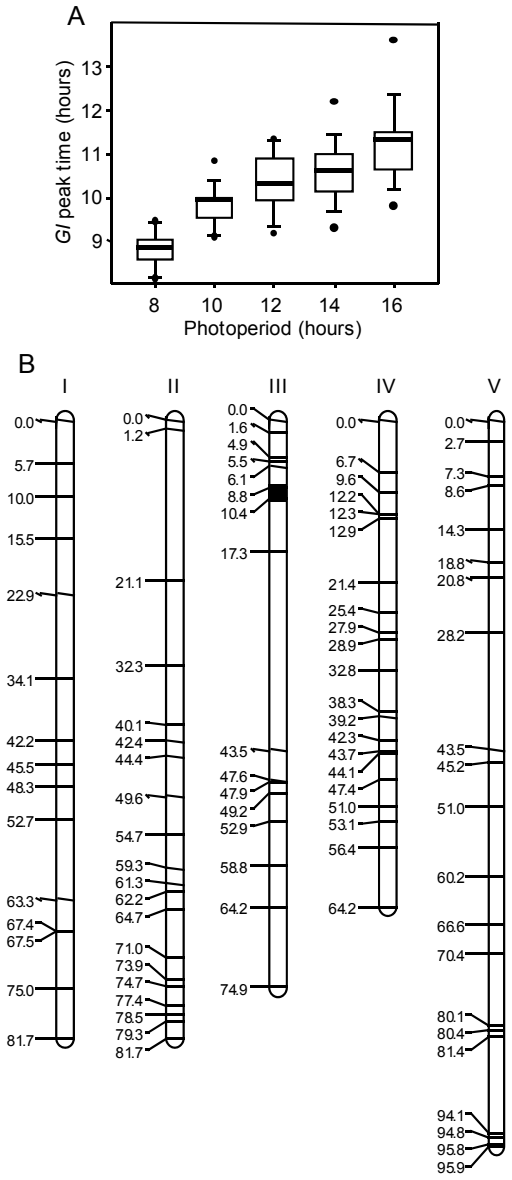

Fig. S3. Phenotypic and genotypic analysis of the Col-0 X Lip-0 *GI::LUC* F2 population. (*A*) Distribution of *GI* peak time measured in Col-0 X Lip-0 F2 progenies grown in five photoperiods. Lower and upper limits of the boxes represent 25th and 75th percentile, error bars represent the 10th and 90th percentile and dots represent the 5th and 95th percentile. Horizontal bars represent the mean. (*B*) Genetic map of the Col-0 X Lip-0 F2 population used for QTL mapping. Genotyping was performed with 96 markers (Sequenom Inc.). Horizontal bars represent markers, and numbers indicate position in cM. Chromosomes are indicated by Roman numerals. The phenotyping of the F2 progenies required selection of the *GI::LUC* transgene, and a strong distortion in the segregation of markers MSQT118 (3679541 bp) and MSQT119 (4141103 bp) revealed the presence of *GI::LUC* on the upper arm of chromosome III (black rectangle). In the original cross the *GI::LUC* transgene was present in the Lip-0 accession, so that all the individuals except one were either heterozygous or homozygous for Lip-0 at the position of MSQT119. No other distortions were detected.

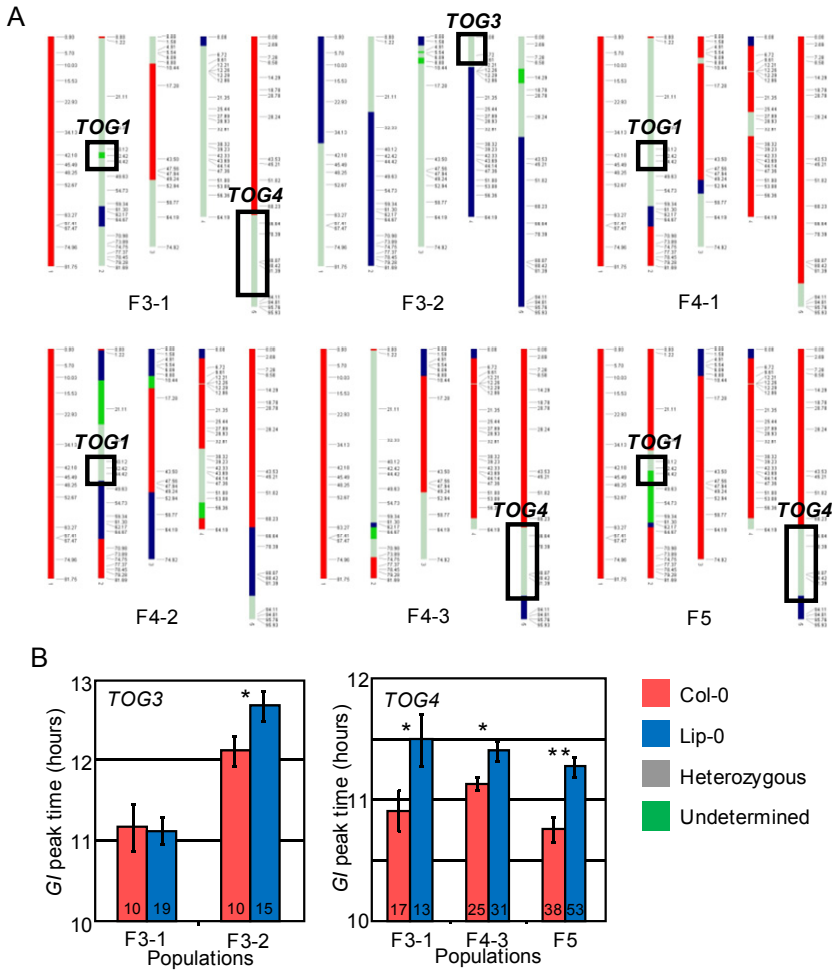

Fig. S4. Detection and confirmation of the *TOG1*, *TOG3* and *TOG4* QTL effects in F3, F4 and F5 populations. (*A*) Genotypes of the parents of the populations used to detect and confirm the QTLs. Boxes indicate the positions of the QTLs. The F3-1 and F3-2 populations were obtained by self-fertilization of F2 plants isolated in the original F2 mapping population. Populations F4-1, F4-2 and F4-3 were obtained after self-fertilization of F3 individuals isolated in F3-1. The F3-1 population was genotyped with the 96 marker set as described for the F2 population in Fig. S3 (Sequenom Inc.). The F5 population was similarly obtained from an F4 plant isolated in F4-3. F4 families were genotyped with in-house markers. (*B*) Markers polymorphic between Col-0 and Lip-0 were designed on chromosomes IV and V to determine the allelic effects of *TOG3* and *TOG4* in the different populations. The effect of *TOG3* was detected in F3-2 but not in F3-1, suggesting that *TOG3* was not segregating in F3-1 and that it was included in the Lip-0 homozygous region at the top of chromosome IV in this population. This region was introgressed in NILs which allowed confirming the effect of *TOG3* (Fig. S5). Because *TOG2* was linked to the *GI::LUC* transgene (Fig. S3), this QTL could not be convincingly confirmed using this approach. (mean ± s.e.m., *n* is indicated on the histograms, *: $p \leq 0.05$, **: $p \leq 0.01$ with a two tailed Student t-test).

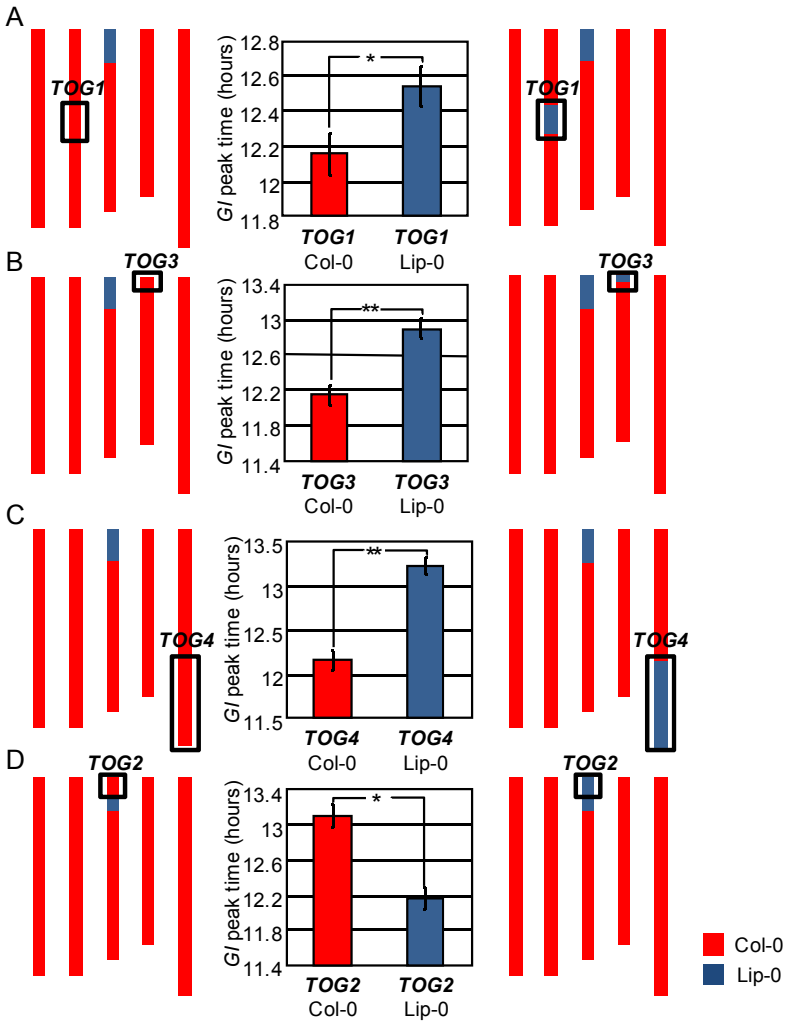

Fig. S5. Confirmation of the effect of (*A*) *TOG1,* (*B*) *TOG3*, (*C*) *TOG4* and (*D*) *TOG2* QTLs in NILs. The peak time of *GI::LUC* expression was determined in the NILs grown in LDs of 16 h. Data were obtained from 5 independent experiments with 12 individuals per genotype per experiment. mean ± s.e.m., p value was determined with a two way ANOVA with genotype and experiment as factors, *: $p \leq 0.05$, **: $p \leq 0.01$. The NILs were generated as described in *SI Material and Methods*, and the sizes of the introgressions are provided in Table S6. For the confirmation of *TOG2*, a recombination event was necessary to combine *TOG2* Col-0 with the *GI::LUC* transgene because in the original cross *GI::LUC* came from the Lip-0 accession and was linked to *TOG2*.

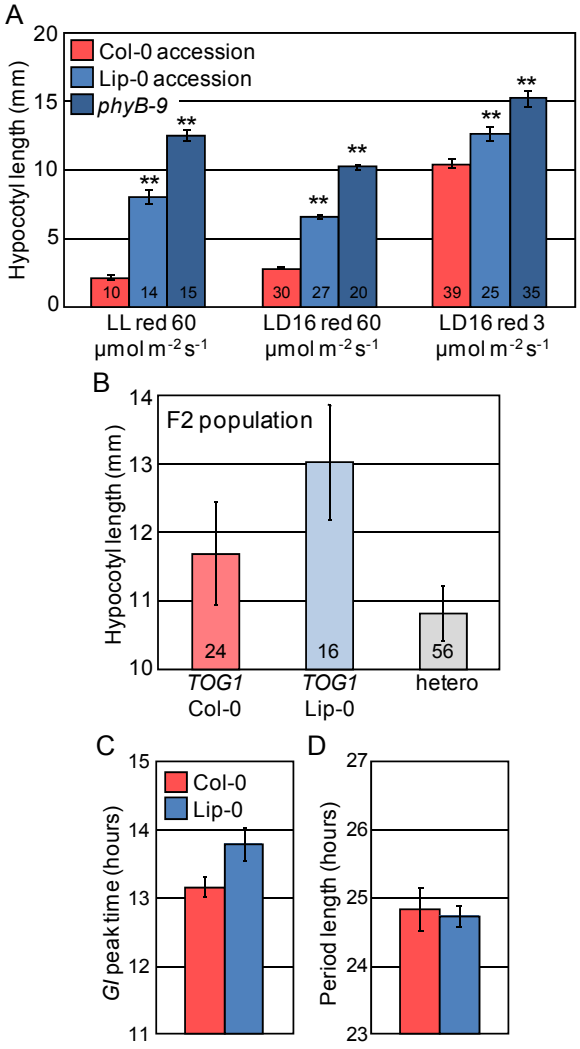

Fig. S6. PHYB activity is altered in the Lip-0 accession and in the F2 population. The Lip-0 genomic sequence of *PHYB* was determined and revealed a 12 nucleotide in frame deletion compared to the Col-0 allele at the 5' end of the coding sequence. This deletion had previously been proposed to reduce PHYB activity (3). (*A*) and (*B*) We confirmed this in our material and experimental conditions. (*A*) Growth phenotype of the Lip-0 accession in constant red light of 60 µmol m^{-2} s^{-1} and in LD 16 h cycles of red light of 3 and 60 µmol m^{-2} s^{-1}. (*B*) Allelic effect of *TOG1* on hypocotyl length in F2 progenies grown LD 16 h cycles of red light of 3 µmol m^{-2} s^{-1}. In (*B*) hypocotyl length of individuals Lip-0 homozygous at *TOG1*, but not of individuals Col-0 homozygous at *TOG1*, were statistically different from the hypocotyls length of heterozygous individuals (two tailed Student t-test). This suggested that *TOG1* Col-0 was the dominant allele. (*C*) Col0 and Lip-0 accessions were entrained in LDs 16 h of red light 60 µmol m^{-2} s^{-1}, and *GI* peak time was determined on day 10 with a CCD camera. (*D*) Plants were then released in constant red light (LL) (60 µmol m^{-2} s^{-1}) and period length was measured. The results of two biological replicates are shown. mean ± s.e.m (n = 4). For (*A*) and (*B*) n is indicated on the bar graphs. mean ± s.e.m., *: $p \leq 0.05$, **: $p \leq 0.01$ with a two tailed Student t-test.

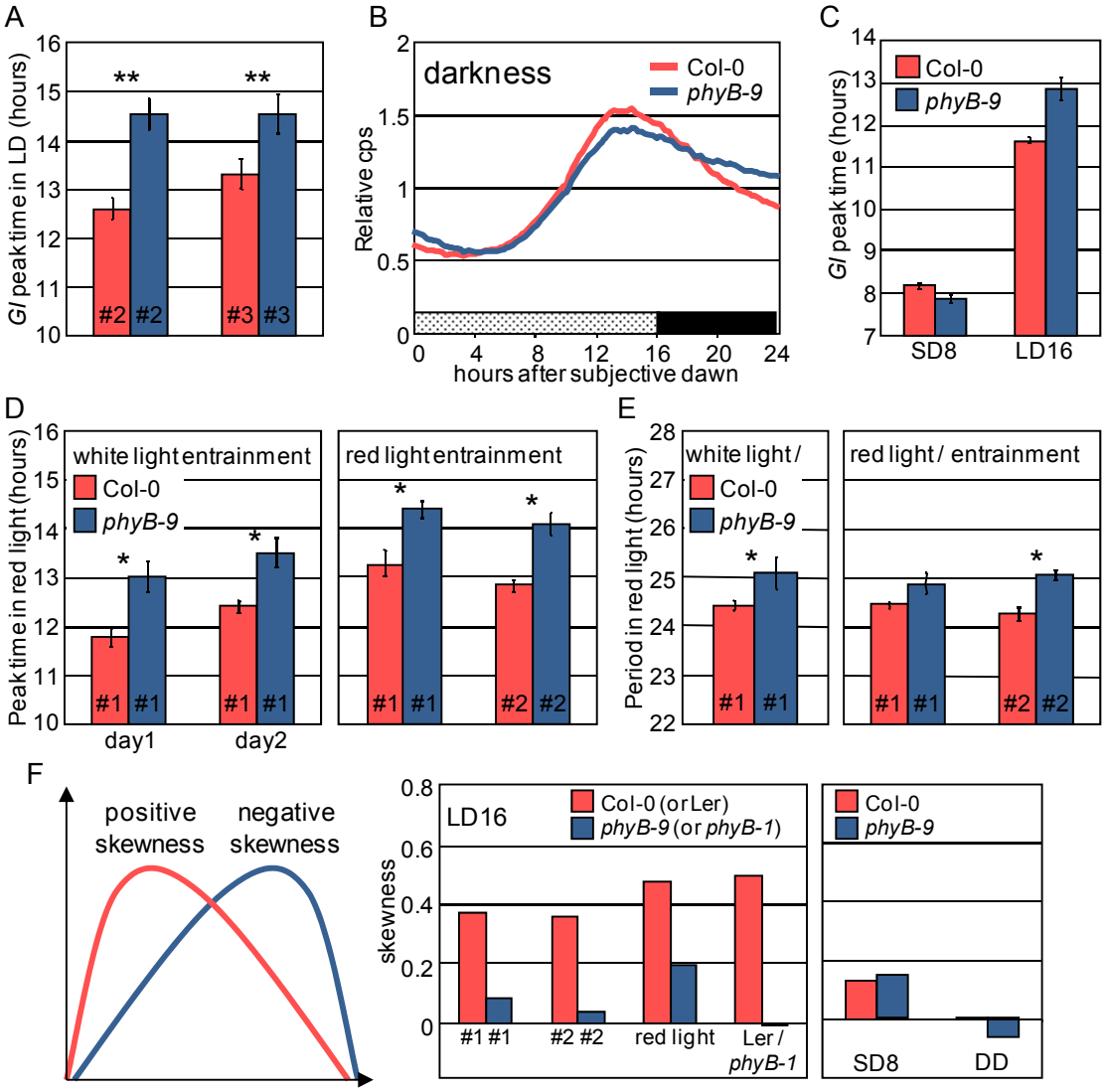

Fig. S7. PHYB activity defines the waveform of *GI* expression in LDs of 16 h. (*A*) Peak time of *GI::LUC* expression measured in independent transgenic lines described elsewhere (35) and not included in Fig. 2. (*B*) Wavefom of *GI::LUC* expression in darkness after entrainment in LDs of 16 h and transfer to DD conditions. (*C*) *GI* peak time measured in Col-0 and *phyB-9* after entrainment in LDs of 16 h and SDs of 8 h (LD16 and SD8) ($n = 32$). (*D*) *GI* peak time measured in red light 60 µmol m^{-2} s^{-1} LDs after entrainment in white light photocycles (results of two consecutive red light LDs are shown) or after entrainment in red light LDs since the first day (results of two transformant lines are shown) ($n = 8$). (*E*) Plants were then released in constant red light (LL) (60 µmol m^{-2} s^{-1}) and period length was determined. (*F*) Skewness of the *GI::LUC* waveforms after entrainment in white light LDs of 16h. The skewness of the curves is also indicated for red light LDs of 16 h, for SDs of 8 h and for darkness as indicated on the figure. mean ± s.e.m., *: $p \leq 0.05$, **: $p \leq 0.01$ with a two tailed Student t-test.

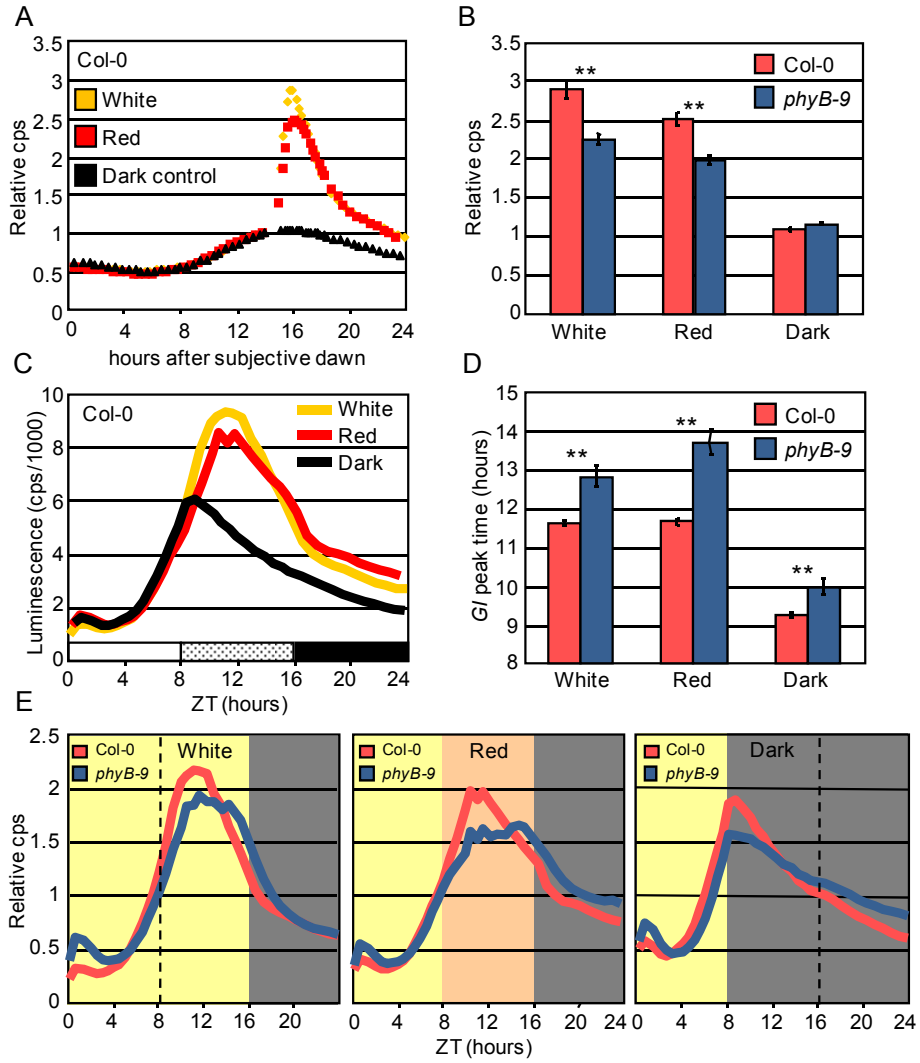

Fig. S8. PHYB activity mediates the acute response to light of *GI* in the evening of a long day. (*A*) Response of Col-0 *GI::LUC* to a 30 minute white or red light pulse applied in the dark 14 hours after subjective dawn. The response was expressed relative to the luminescence measured before the pulse. (*B*) Maximum relative luminescence of Col-0 and *phyB-9* after the light pulse. (*C*) The *GI::LUC* waveform was determined in Col-0 during a LD of 16 h after plants were shifted at ZT 8 h either to 60 µmol m^{-2} s^{-1} red light, either to darkness, or left in white light. Luminescence is expressed in cps = counts per second. (*D*) *GI* peak time measurements in Col-0 and *phyB-9* and (*E*) *GI::LUC* waveform after the shift to different light qualities at ZT 8 h. *n* = 12-24. mean ± s.e.m., *: $p \leq 0.05$, **: $p \leq 0.01$ with a two tailed Student t-test.

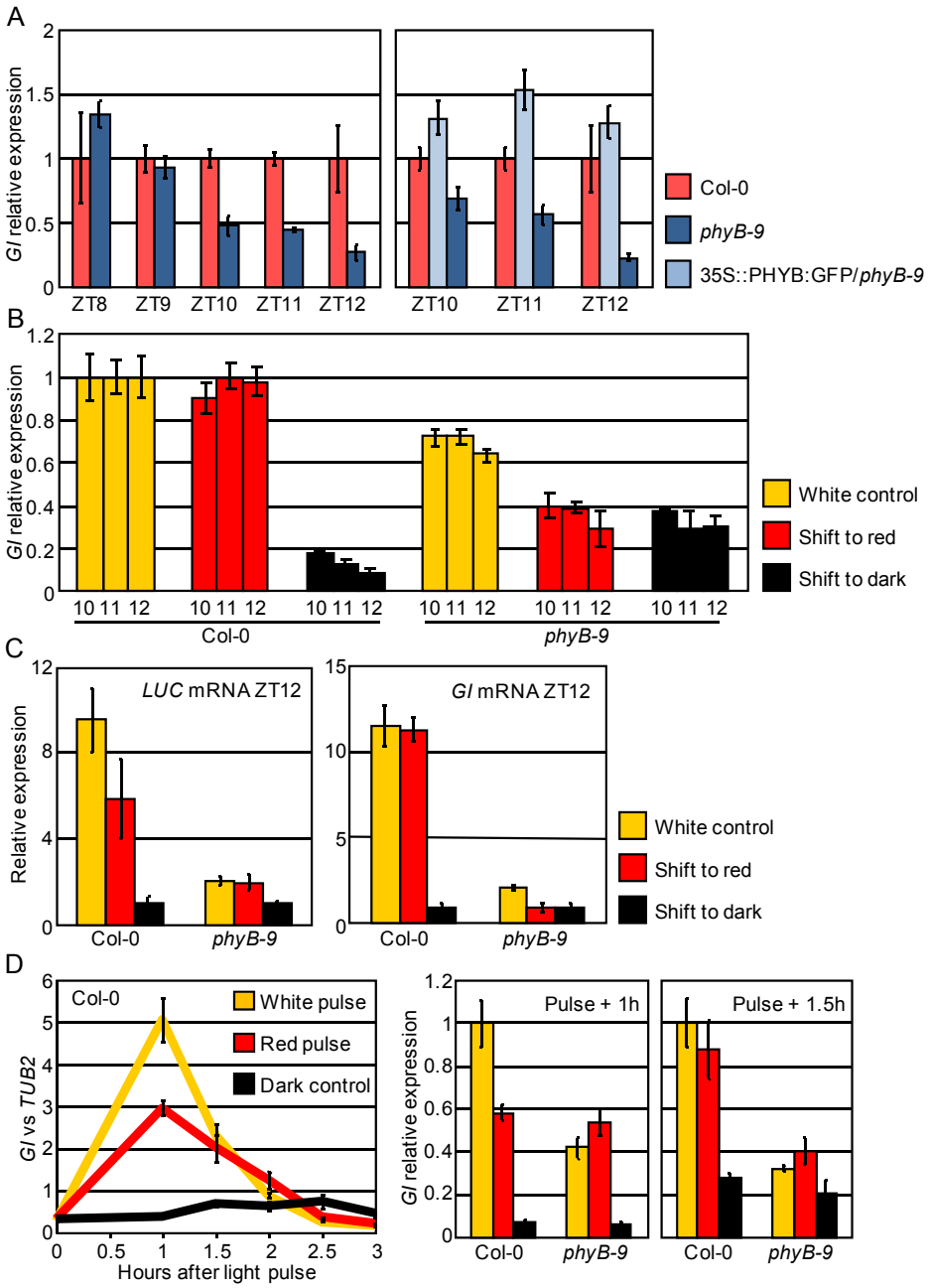

Fig. S9. Reduced PHYB activity alters *GI* expression levels in the evening of an LD of 16 h. (*A*) *GI* mRNA levels determined by qRT PCR in Col-0, *phyB-9* and *35S::PHYB:GFP phyB-9* samples harvested in the evening of a LD of 16 h at the indicated times. *35S::PHYB:GFP* was previously described in (35). (*B*) *GI* mRNA levels determined by qRT-PCR in parallel to the experiment described in Fig. S8*C*. Samples were harvested after the shift to the different light conditions at ZT 10, 11 and 12 h. (*C*) *LUC* mRNA and *GI* mRNA levels determined at ZT 12 h in the same samples than in (*B*) and expressed relatively to the dark control. (*D*) *GI* mRNA levels in samples harvested in parallel to the experiment described in Fig. S8*A*. Results for Col-0 and *phyB-9* were compared 1 and 1.5 hours after the pulse. mean ± s.d. of four technical replicates.

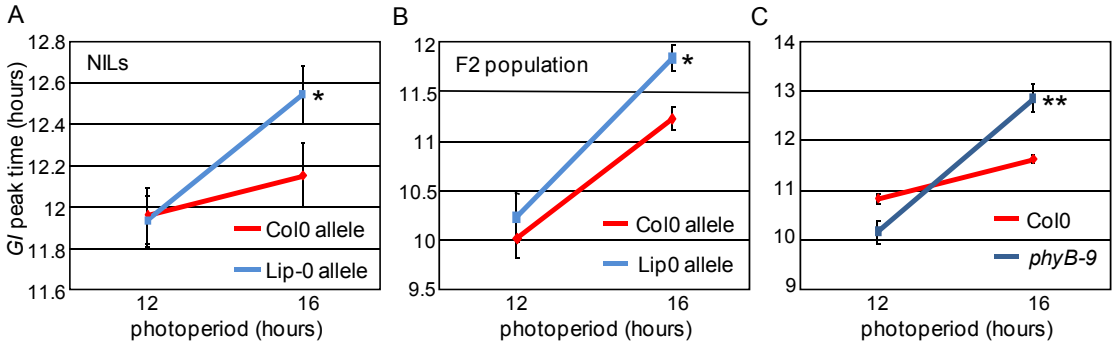

Fig. S10. The *PHYB* Col-0 allele advances *GI* peak time specifically in LDs of 16 h. *GI* peak time of expression was determined in LDs of 12 h and compared to the results in LDs of 16 h for (*A*) the NILs in which the *TOG1* allelic effect had been confirmed (Fig. S5*A*), (*B*) the Col-0 X Lip-0 GI::LUC F2 population, and (*C*) Col-0 and the *phyB-9* mutant. The delay in *GI* peak time due to reduced PHYB activity was not detected in LDs of 12 h. (*A*) Data are the mean of five biological replicates with n = 12 per experiment. (*B*) *GI::LUC* expression was monitored in 80 to 90 F2 individuals and subsequently genotyped for allelic variation at *PHYB*. The average peak time for Col-0 and Lip-0 homozygous plants was determined. (*C*) n = 32. mean ± s.e.m.. * $p \leq 0.05$. p was determined with a two tailed Student t-test (α=0.05).

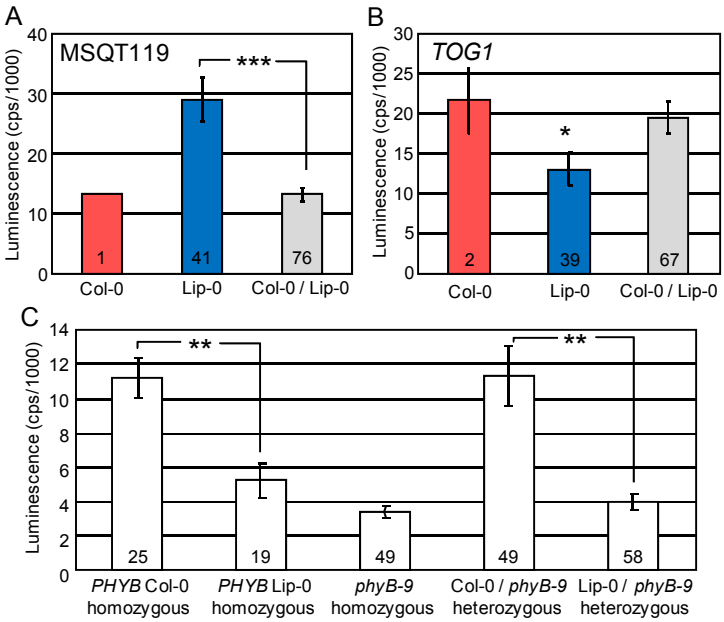

Fig. S11. *PHYB* is the gene underlying *TOG1*. (*A*) Allelic effect of marker MSQT119 on *GI::LUC* expression levels at peak time in the Col-0 X Lip-0 *GI::LUC* F2 population. MSQT119 is linked to *GI::LUC* (Fig. S3), so that the allelic effect of this marker reflects the dosage of the transgene. Individuals that are Lip-0 homozygous at MSQT119 displayed approximately 2 fold higher LUC activity than individuals heterozygous at MSQT119. This result shows that the variation of *GI::LUC* expression level at peak time can be associated to allelic variation at specific loci. *n* is indicated inside the bars of the histogram. (*B*) *GI::LUC* expression in Col-0 X Lip-0 F2 progenies heterozygous, homozygous Col-0, or homozygous Lip-0 at *TOG1*. Individuals Lip-0 homozygous at *TOG1* displayed significantly lower *GI::LUC* expression levels than individuals Col-0 homozygous or heterozygous at this loci. Moreover, *GI::LUC* expression was not significantly different between individuals Col-0 homozygous or heterozygous at *TOG1*, showing that the Col-0 allele was dominant. (*C*) Allelism test performed by crossing the NILs in which the *TOG1* allelic effect had been confirmed (Fig. S5*A*) to the *phyB-9* mutant. The effect of the segregating *PHYB* alleles was determined in families resulting from these crosses and in which the *GI::LUC* transgene located on top of chromosome III had previously been made homozygous. In this experiment, the individuals were first scored for *GI::LUC* activity and subsequently genotyped for the different *PHYB* alleles to determine the allelic combination present in each seedling. *n* is indicated in the bars of the histogram. mean ± s.e.m. *: $p \leq 0.05$, **: $p \leq 0.01$, and ***: $p \leq 0.001$ with a two tailed Student t-test.

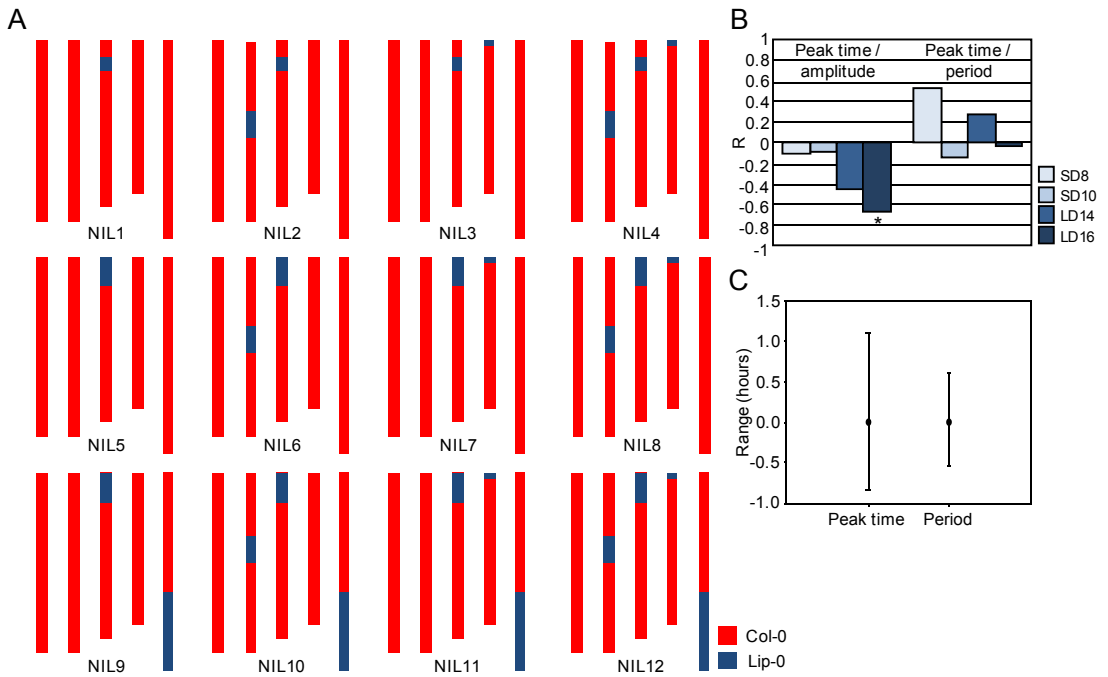

Fig. S12. Natural *TOG* alleles modify the timing and the evening expression level of *GI* expression. (*A*) Schematic representation of the genotypes of the 12 NILs bearing combinations of *TOG1-4* introgressions. (*B*) Correlations between *GI* peak time and *GI* maximum expression levels, and between *GI* peak time and period length in the NILs grown in four photoperiods. Period length was determined in DD after entrainment in the different light regimes. The Pearson correlation coefficient (R) indicates the strength of the correlations, 1 and -1 indicating perfect positive and negative correlations respectively. (*C*) Range of *GI* peak time of expression and period length in the NILs entrained in 60 µmol m^{-2} s^{-1} red light photocycles. Period length was determined in constant red light after entrainment (n = 8). mean ± s.e.m., *: $p \leq 0.05$, **: $p \leq 0.01$ with a two tailed Student t-test.

Table S1. List of Arabidopsis accessions used in this study.

	GI peak time (hours)					*GI* period length (hours)				
	SD8	SD10	LD12	LD14	LD16	SD8	SD10	LD12	LD14	LD16
Aa-0	8.84	9.67	9.97	11.09	11.10	27.71	27.97	27.84	28.00	28.01
Ak-1	8.59	9.84	10.43	10.73	11.20	26.58	27.52	27.38	27.80	27.28
An-2	8.00	9.53	9.55	9.56	9.79	25.23	27.23	26.44	26.04	26.21
Ba-1	8.56	9.73	9.98	10.31	10.78	27.85	28.15	27.67	27.71	27.35
Bay0	8.46	8.86	9.93	10.06	11.29	29.35	29.73	27.85	28.64	28.38
Bch-1	8.57	9.41	10.52	10.79	11.52	27.41	27.40	26.24	26.63	26.84
Bd-0	8.89	10.30	10.89	11.33	11.57	26.96	26.89	26.73	26.85	26.77
Be-2	8.64	9.94	10.14	10.37	10.74	28.24	27.99	26.98	28.14	28.13
Berkeley	8.61	9.38	9.52	10.23	10.21	26.23	26.99	27.84	27.43	27.32
Bla-3	8.76	9.46	10.26	10.61	11.16	28.70	27.70	28.40	28.18	28.06
Br-0	8.45	9.59	9.64	9.76	10.34	27.58	26.49	26.48	27.75	27.54
Bs-1	8.56	9.69	10.58	10.58	11.27	28.43	27.28	28.69	28.99	28.89
Bs-2	8.15	9.53	9.65	10.35	10.84	27.98	27.87	26.84	28.18	26.45
Bs-5	8.71	9.38	9.91	10.24	10.59	26.86	28.20	27.92	27.85	27.75
Bsch-0	8.63	9.36	10.28	10.33	10.74	27.55	27.93	26.94	27.57	27.99
Bsch-2	8.69	9.28	9.42	9.43	9.83	27.95	28.06	26.79	25.94	27.22
Bu-0	9.22	10.42	11.12	11.32	12.35	27.11	27.69	28.14	28.38	27.98
Bu-2	8.79	9.59	10.15	10.81	10.83	27.28	27.58	28.18	28.02	27.70
Bur-0	8.03	9.14	9.72	9.96	10.24	26.44	26.26	26.43	27.13	27.71
C24	8.51	9.10	9.60	9.88	10.04	26.56	26.68	26.94	28.48	28.86
Cen-0	8.60	9.76	10.51	10.74	11.05	26.45	27.04	26.84	27.05	27.05
Chi-0	8.60	9.75	9.93	10.85	11.25	26.57	26.60	26.20	26.97	26.82
Cl-0	8.47	9.55	10.60	10.79	11.15	27.88	29.18	28.17	29.67	26.56
Co-1	8.22	9.44	9.73	10.08	10.49	28.37	27.14	28.79	28.24	28.38
Col-0	8.64	9.67	10.10	10.36	11.33	26.65	26.47	26.46	26.92	26.09
Col-2	8.68	9.86	10.09	10.31	10.92	27.53	27.96	26.99	27.32	27.09
Col-3	8.74	9.59	9.98	10.33	10.79	26.57	25.96	26.43	27.95	26.70
Ct-1	8.64	9.15	9.97	10.58	11.04	27.64	28.86	28.00	27.95	27.05
Da-0	8.65	9.93	10.16	10.52	10.63	26.62	29.08	25.46	26.84	26.95
Da(1)-12	8.46	8.74	9.46	10.33	10.26	26.27	26.69	27.04	26.34	26.96
Db-0	8.73	10.22	10.69	11.33	11.89	27.95	27.47	28.64	27.75	28.50
Di-G	9.04	10.08	11.54	12.09	12.38	28.35	29.43	28.79	28.27	28.48
Di-M	8.60	8.92	9.04	9.93	9.98	28.41	27.24	28.84	28.87	28.65
Dr-0	8.51	9.43	10.50	10.46	11.42	28.48	28.92	29.68	28.53	28.07
Dra-0	10.50	10.62	11.08	11.54	11.50	24.32	26.26	25.28	26.38	25.12
Edi-0	8.76	10.37	10.38	10.42	10.56	27.66	26.81	27.69	27.17	28.11
Ei	8.41	8.95	9.18	9.57	10.19	26.15	26.79	27.29	27.29	27.56
Ei-2	8.65	9.42	9.66	9.98	10.58	27.20	27.00	27.57	27.68	26.26
Eil-0	8.66	9.61	10.34	10.44	11.49	28.68	28.52	28.44	29.52	29.42
El-0	8.64	9.54	9.68	9.65	10.25	26.51	27.36	26.96	27.79	27.12
En-2	8.51	9.92	10.27	10.54	10.57	27.12	27.67	26.71	26.79	27.71
En-D	8.57	9.82	9.78	9.95	10.86	27.13	27.74	26.71	28.10	27.30
En-T	8.85	9.36	10.33	10.77	10.93	26.90	27.10	27.74	27.31	28.01
Est	8.15	9.40	9.96	10.28	10.49	28.65	26.72	28.44	28.92	29.24
Et-0	8.55	9.89	10.10	10.27	10.79	26.67	27.74	27.84	27.29	28.01
Fr-4	8.93	9.31	10.23	11.03	11.05	26.57	27.01	27.25	26.76	26.79
Gr	8.46	9.45	9.57	9.69	10.76	27.35	26.87	25.74	26.43	25.38
Gre-0	8.68	9.86	10.03	11.04	11.83	26.48	27.46	27.77	27.55	27.28
H55	8.70	10.20	10.50	11.30	11.37	27.96	27.44	27.64	24.97	27.78
Hi-0	8.79	9.89	10.47	10.78	11.03	26.66	26.88	25.51	25.91	25.88
Hs-0	8.92	9.96	9.94	10.90	11.27	28.29	27.76	28.09	28.29	28.58
Je54	9.49	10.32	10.78	11.37	11.47	27.70	27.76	28.29	28.07	28.04
Lc-0	8.56	9.66	10.68	10.87	11.29	27.09	27.21	27.76	28.84	28.88
Li-1	8.77	10.13	10.57	10.55	11.09	26.54	27.01	27.09	27.01	26.04
Lip-0	8.81	10.20	11.05	11.93	12.08	28.22	28.65	28.56	28.13	28.56
Lm-2	8.60	9.89	10.29	10.85	11.38	27.33	28.00	26.93	28.09	27.53

Lu-1	8.36	9.86	10.42	10.60	11.96	26.65	26.40	27.54	28.38	27.11
Mt-0	8.62	9.71	9.69	10.77	11.12	27.74	27.24	28.22	28.30	28.37
Nd	8.50	9.45	10.05	10.52	11.29	27.46	27.66	27.27	27.44	28.36
No-0	9.13	10.22	10.73	11.36	11.71	28.74	28.68	28.76	29.19	28.30
Ob-0	8.53	9.95	10.00	10.68	11.05	27.42	28.01	27.73	28.18	27.40
Oy	8.69	10.21	10.80	10.92	11.30	27.15	27.35	28.71	28.44	28.47
Petergof	8.51	9.64	9.62	10.25	11.15	27.51	28.30	27.76	28.10	27.77
PHW	8.87	9.94	10.36	11.28	11.59	26.53	26.36	27.68	28.45	27.93
RLD-1	8.61	9.45	10.04	10.00	10.73	26.40	29.39	27.87	28.69	27.67
Rsch-0	8.77	9.53	10.14	10.69	10.65	26.37	27.63	27.93	27.67	27.88
Rubez-1	8.30	9.39	9.58	10.24	10.57	28.41	28.79	28.61	27.84	28.02
S96	8.92	9.84	10.93	12.07	12.17	28.17	27.45	25.46	27.70	27.03
Sha	8.04	9.07	9.69	10.70	11.15	27.68	28.21	27.28	26.74	27.09
Sn(5)-1	8.79	9.37	10.08	10.42	10.53	29.31	24.21	28.09	28.22	28.23
Sol-0	8.74	9.35	9.39	10.09	10.60	28.60	26.23	28.55	28.50	28.07
Ta	8.48	10.30	10.60	10.84	11.75	30.20	28.44	29.49	29.86	28.39
Tsu-0	8.42	9.51	9.55	10.01	10.19	28.32	27.34	27.78	28.17	27.53
Wil	8.71	9.77	10.84	10.88	11.10	28.34	27.49	28.08	28.68	28.49
Ws-0	8.40	9.66	9.86	9.95	10.22	26.67	26.35	28.15	27.99	25.93
Yo	8.27	9.20	9.79	9.84	11.31	26.78	26.69	27.08	27.03	26.57

Average *GI* peak time during the day and period length in constant darkness is given for every accession in the five photoperiods tested.

Table S2. Statistical analysis of *GI* peak time and period length in the accessions.

***GI* peak time**

LD16	Df	SS	MS	F	% Exp	P
Accession	38	458.24	12.06	28.203	26.9	<1E-15
Accession/Trans	57	366.38	6.43	15.033	21.5	<1E-15
Residuals	2055	878.66	0.43			
LD12	Df	SS	MS	F	% Exp	P
Accession	38	503.26	13.24	31.756	30.6	<1E-15
Accession/Trans	57	293.86	5.16	12.362	17.9	<1E-15
Residuals	2034	848.28	0.42			
SD8	Df	SS	MS	F	% Exp	P
Accession	38	116.79	3.07	12.525	16.8	<1E-15
Accession/Trans	55	103.6	1.88	7.676	14.9	<1E-15
Residuals	1940	476.05	0.25			

Period length

LD16	Df	SS	MS	F	% Exp	P
Accession	37	1449.8	39.2	10.814	17.2	<1E-15
Accession/Trans	49	536.3	10.9	3.0206	6.4	<1E-15
Residuals	1778	6442.4	3.6			
LD12	Df	SS	MS	F	% Exp	P
Accession	37	1762.9	47.6	11.6162	17.4	<1E-15
Accession/Trans	52	766.2	14.7	3.5926	7.6	<1E-15
Residuals	1854	7604.4	4.1			
SD8	Df	SS	MS	F	% Exp	P
Accession	37	1288	34.8	8.4336	13.9	<1E-15
Accession/Trans	50	792.7	15.9	3.8408	8.5	<1E-15
Residuals	1747	7211.2	4.1			

Df: degrees of freedom. SS: sums of squares. MS: Mean squares. F: F ratio. P: p value. % Exp: percentage of variance explained. Trans: transgenic line. Accession/Trans: factor "transgenic line" nested within factor "accession". We tested the contributions of the accessions and of the insert position (transgenic line) to variation of *GI* peak time and period length with an ANOVA using accession and transgenic line nested within accession as factors. The statistical tests were performed with the data from the 39 accessions for which at least two transgenic lines had been scored (see *Methods*).

Table S3. Analysis of the technical variability observed for *GI* peak time.

	Col-0 X Lip-0 F2 population		Accessions							
			experiment 1		experiment 2		experiment 3		experiment 4	
	plate 1	***plate 2***	Col-0	Lip-0	Col-0	Lip-0	Col-0	Lip-0	Col-0	Lip-0
Mean	***11.06***	***11.69***	10.55	11.29	10.72	11.68	10.81	12.01	10.97	12.72
s.d.	***0.77***	***0.98***	0.46	0.43	0.68	0.54	0.51	0.93	0.55	0.48
n	***48***	***48***	48	47	36	36	32	32	32	32

The variation of *GI*::*LUC* peak time of expression was analyzed in the Col-0 X Lip-0 *GI*::*LUC* F2 population, and compared with the variation observed in Col-0 *GI*::*LUC* and Lip-0 *GI*::*LUC* populations of a similar size. Plate 1 and plate 2 refer to independent experiments in which the Col-0 X Lip-0 *GI*::*LUC* F2 population was tested. Four biological replicates (experiments 1 to 4) of Col-0 *GI*::*LUC* and Lip-0 *GI*::*LUC* populations were analyzed. Data from LDs of 16 h were used for these comparisons as maximum variation between accessions and within the F2 population were detected in this condition. This analysis shows that there was more phenotypic variability within the F2 population than within populations of Col-0 *GI*::*LUC* and Lip-0 *GI*::*LUC*. Therefore, technical variability alone did not account for the variation observed in the F2. Further statistical treatments of these data are presented in Table S4. s.d.: standard deviation. *n*: number of individuals per experiment.

Table S4. Statistical analysis of *GI::LUC* peak time of expression in Col-0 and Lip-0.

	Df	F	P	% Exp
Genotype	1	250.685	<0.001	39.64899
Experiment	3	30.525	<0.001	14.48395
Residuals	290			45.86706

Df: degrees of freedom. F: F ratio. P: p value. % Exp: percentage of variance explained. Data were obtained from four biological replicates in which Col-0 *GI*::*LUC* and Lip-0 *GI*::*LUC* were grown in LDs of 16 h, as previously described in Table S3. The F ratios and p values were determined with a two way ANOVA using genotype and experiment as factors.

Table S5. QTL detection summary in the F2 population.

	Chromosome	Position cM	LOD score	% Expl	Additive effect	QTL name
GI peak time LD1	2	40.12	2.59	7.4	-0.42	*TOG1*
	3	1.58	3.54	10.2	0.46	*TOG2*
	4	0	0.53	1.4	0.17	*TOG3*
	5	60.23	1.22	3.4	-0.23	*TOG4*
GI peak time LD2	2	40.12	2.52	7.1	-0.30	*TOG1*
	3	1.58	1.78	4.9	0.36	*TOG2*
	4	0.00	2.32	6.6	0.17	*TOG3*
	5	60.23	0.62	1.6	-0.26	*TOG4*

cM: centimorgan. LOD: Likelihood of odds. % Expl: percentage of variance explained. For the additive effect, negative values indicate that the Lip-0 allele delays *GI* peak time. LD1 and LD2: first and second consecutive LD cycles of 16 h light / 8 h dark. Note that the effects of *TOG3* and *TOG4* were not significant in the F2 population but a LOD peak was detected at *TOG3* in LD2, and a weak but consistent effect was detected at *TOG4* in both LDs. Based on these results the effects of *TOG3* and *TOG4* were further tested in F3 families and these experiments confirmed *TOG3* and *TOG4* (Fig. S4). All the QTLs were finally confirmed in NILs (Fig. S5).

Table S6. Size of the *TOG* introgressions in the NILs presented in Fig. S5.

			Introgression				
interval	polymorphism		*TOG1*	*TOG2*	*GI::LUC* transgene	*TOG3*	*TOG4*
large interval	upper	position	6402846	-	2236791	-	18888298
		reference	CIW3	-	ossowski_455674	-	PERL1058386
	lower	position	10032183	4141096	4141096	269026	-
		reference	PERL0356500	PERL0446897	PERL0446897	FRI	-
	interval size	size in bp	3629337	4141096	1904305	269026	9821054
small interval	upper	position	7203681	-	3679535	-	17154448
		reference	PERL0336650	-	MASC01999	-	PERL1026858
	lower	position	9529916	3679535	4141096	195281	-
		reference	PERL0353940	MASC01999	PERL0446897	PERL0659066	-
	interval size	size in bp	2326235	3679535	461561	195281	8087204

The positions and reference numbers of the polymorphisms that define the limits of the introgressions are indicated. Upper and lower polymorphisms define the upper and lower limits of the intervals. The large interval is defined by the two upper and lower polymorphisms that fall outside the introgression. The small interval is defined by the two upper and lower polymorphisms that fall inside the introgression. The upper limits of *TOG2* and *TOG3* are the top of chromosome III and IV, respectively, and the lower limit of *TOG5* is the bottom of chromosome V, which is why there is no polymorphism information at these positions. The *GI::LUC* transgene came from the Lip-0 accession in the original cross and was linked to *TOG2* (Fig. S3). Therefore, the table also provides the size of the introgression when the transgene was isolated from *TOG2* Lip-0. Marker CIW3 is available on the TAIR website (www.arabidopsis.org). The FRI marker in Col-0 was described in (4). Reference numbers of the SNPs were found on the TAIR website.

Table S7. *GI* peak time, *GI* expression level at peak time (*GI* max) and period length in DD measured in the NILs.

***GI* peak time (h)**	SD8	SD10	LD14	LD16
NIL1	8.758 ± 0.0478	10.654 ± 0.0493	12.863 ± 0.101	13.095 ± 0.103
NIL2	8.736 ± 0.0478	10.68 ± 0.0489	12.45 ± 0.101	12.882 ± 0.103
NIL3	8.703 ± 0.0493	10.714 ± 0.0489	12.835 ± 0.102	13.348 ± 0.103
NIL4	8.698 ± 0.0478	10.698 ± 0.0493	12.551 ± 0.103	13.023 ± 0.103
NIL5	8.852 ± 0.0478	10.667 ± 0.0489	12.351 ± 0.101	12.155 ± 0.103
NIL6	8.857 ± 0.0482	10.68 ± 0.0493	12.362 ± 0.114	12.543 ± 0.103
NIL7	8.887 ± 0.0478	10.762 ± 0.0489	12.829 ± 0.101	12.899 ± 0.103
NIL8	8.808 ± 0.0478	10.813 ± 0.0489	12.935 ± 0.101	12.88 ± 0.103
NIL9	8.814 ± 0.0486	10.682 ± 0.0489	12.774 ± 0.101	13.22 ± 0.104
NIL10	8.883 ± 0.0478	10.829 ± 0.0489	12.81 ± 0.103	13.128 ± 0.105
NIL11	8.901 ± 0.0478	10.637 ± 0.0557	12.881 ± 0.101	13.381 ± 0.103
NIL12	8.843 ± 0.0482	10.626 ± 0.0489	12.447 ± 0.101	12.885 ± 0.103
n / genotype	**60**	**60**	**60**	**60**
p	**0.012**	**0.06**	**<0.001**	**<0.001**

***GI* max (cps)**	SD8	SD10	LD14	LD16
NIL1	2487.267 ± 328.56	5324.133 ± 445.704	4220 ± 369.05	5931.507 ± 432.358
NIL2	3270.133 ± 328.56	3789.133 ± 445.704	4865.533 ± 369.05	6210.933 ± 423.962
NIL3	3773 ± 328.56	5164.533 ± 445.704	5435.333 ± 369.05	6982.387 ± 432.358
NIL4	3236.4 ± 328.56	4545.667 ± 445.704	6126.224 ± 378.713	7382.8 ± 432.358
NIL5	4729.8 ± 328.56	6943.805 ± 453.411	6340.158 ± 375.434	8507.897 ± 427.799
NIL6	3748.267 ± 328.56	4270.8 ± 445.704	6354.792 ± 416.355	7772 ± 423.962
NIL7	2677.6 ± 328.56	4469.467 ± 445.704	5020.641 ± 375.434	5859.194 ± 427.799
NIL8	2536.2 ± 328.56	4449.667 ± 445.704	5086.133 ± 369.05	6742.2 ± 423.962
NIL9	2653.267 ± 328.56	4596.8 ± 445.704	4371.733 ± 369.05	5371.6 ± 423.962
NIL10	3155.2 ± 328.56	3797.267 ± 445.704	5206.733 ± 369.05	6337.267 ± 423.962
NIL11	2688.733 ± 328.56	3423.588 ± 502.825	4742.933 ± 369.05	5801.4 ± 423.962
NIL12	2483.333 ± 328.56	3584.533 ± 445.704	4054.733 ± 369.05	5473.236 ± 427.799
n / genotype	**60**	**60**	**60**	**60**
p	**<0.001**	**<0.001**	**<0.001**	**<0.001**

period length (h)	SD8	SD10	LD14	LD16
NIL1	26.396 ± 0.264	26.151 ± 0.303	25.958 ± 0.372	25.754 ± 0.422
NIL2	26.236 ± 0.259	26.038 ± 0.303	25.801 ± 0.345	25.119 ± 0.314
NIL3	26.027 ± 0.253	26.083 ± 0.309	25.373 ± 0.364	25.103 ± 0.314
NIL4	25.703 ± 0.261	25.305 ± 0.298	25.083 ± 0.368	24.946 ± 0.32
NIL5	26.215 ± 0.256	26.071 ± 0.298	25.637 ± 0.354	25.405 ± 0.297
NIL6	26.417 ± 0.263	26.03 ± 0.303	25.948 ± 0.391	25.994 ± 0.308
NIL7	25.862 ± 0.251	25.989 ± 0.309	26.001 ± 0.357	25.554 ± 0.305
NIL8	26.603 ± 0.28	26.231 ± 0.309	26.102 ± 0.361	26.45 ± 0.317
NIL9	26.452 ± 0.253	26.534 ± 0.318	26.945 ± 0.351	26.023 ± 0.309
NIL10	26.516 ± 0.253	26.4 ± 0.306	25.836 ± 0.345	25.654 ± 0.33
NIL11	26.73 ± 0.268	26.212 ± 0.361	26.298 ± 0.345	25.753 ± 0.297
NIL12	26.57 ± 0.258	27.099 ± 0.309	26.131 ± 0.348	25.768 ± 0.309
n / genotype	**60**	**60**	**60**	**60**
p	**0.148**	**0.043**	**0.07**	**0.037**

Least Square means ± s.e.m. are shown. *n* denotes number of individuals assayed per NIL per photoperiod. Data were obtained from 5 independent biological replicates per condition. 12 individuals were assayed per genotype per experiment (2880 plants in total). The contribution of genotypic variation to variation of the phenotype was determined with two way ANOVA with genotype and experiment as factors. p indicates statistical significance of the F ratio.

Table S8. Primers used for qRT PCR.

gene	forward primer	reverse primer
GI	TGGTTTCCTCTTGGATTCAT	CTGTTCAGACGTTCAAAGGC
PIF4	CGGAGTTCAACCTCAGCAGT	ACCGGGATTGTTCTGAATTG
LUC	AAGCGGTTGCCAAGAGGTTCC	CGCGCCCGGTTTATCATC
TUB2	ACACCAGACATAGTAGCAGAAATCAAG	ACTCGTTGGGAGGAGGAACT
IPP2	GTATGAGTTGCTTCTGGAGCAAAG	GAGGATGGCTGCAACAAGTGT